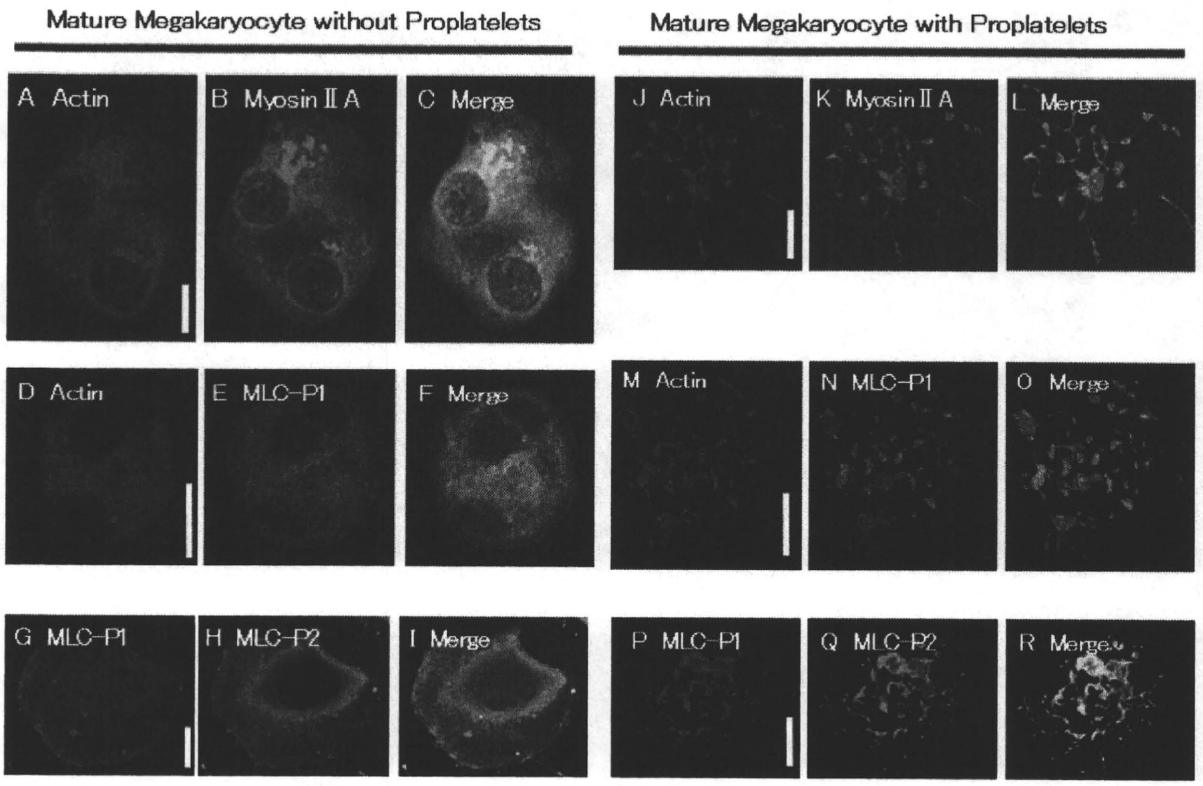

Fig. 2. Localization of actin, myosin IIA, MLC-P1, and MLC-P2 of mature MKs with or without proplatelets. Mature MKs with (right) or without (left) proplatelets were fixed, permeabilized, and incubated with respective antibodies. Stained cells were observed by confocal laser microscopy. Left side: (A) actin (red), (B) myosin IIA (green), (C) merge of actin (A), and myosin IIA (B). (D) Actin (red), (E) MLC-P1 (green), (F) merge of actin (D), and MLC-P1(E). (G) MLC-P1 (red), (H) MLC-P2 (green), (I) merge of MLC-P1 (G), and MLC-P2 (H). Right side: (J) actin (red), (K) myosin IIA (green), (L) merge of actin (J), and myosin IIA (K). (M) Actin (red), (N) MLC-P1 (green), (O) merge of actin (M), and MLC-P1(N). (P) MLC-P1 (red), (Q) MLC-P2 (green), (R) merge of MLC-P1 (P), and MLC-P2 (Q). Cell nuclei were also stained with DAPI (blue). Scale bar, 10 μm. (For interpretation of the references to color in this figure legend, the reader is referred to the web version of this article.)

MK cell body, as well as slightly expressed in the proplatelet shafts (Fig. 2K). Both MLC-P1 and MLC-P2 were diffusely located in the entire cytoplasm (Fig. 2N, P, and Q). In addition, MLC kinase was expressed diffusely in the PPF and MK cell body, and strongly expressed in the periphery of platelet-sized beads (data not shown). And finally, Rho-kinase was expressed diffusely in the PPF and MK cell body (data not shown).

Localization of actomyosin in the retracted PPF following calyculin A treatment

After 5 min of calyculin A treatment, the presence of actomyosin in the retracted PPF was investigated (Fig. 3). Actin was diffusely expressed in the retracted MK, with strong expression in the periphery of the retracted cell; however, there was no expression within the nucleus (Fig. 3A, D, and G). In the retracted cells, myosin IIA was diffusely expressed (Fig. 3B) and MLC-P1 showed strong expression in the periphery of the retracted cell, which was almost the same site of actin localization (Fig. 3E and G). In addition, MLC-P2 was diffusely expressed in the retracted cell, with strong expression in the perinuclear lesion (Fig. 3H); however, compared to MLC-P1 localization, MLC-P2 existed in the inner area of the retracted cell.

Discussion

The molecular mechanisms that are involved in the PPF of MKs have not been previously described. Since PPF coincides with dramatic morphological changes, actomyosin has been thought to participate in the generation of proplatelets. Indeed, the actin cytoskeleton may play an important role in PPF, since cytoplasmic polymerized actin is associated with demarcation membranes, and actin is highly aggregated to the PPF of MKs [16]. In addition, the actin cytoskeleton is important in platelet function, since it regulates platelet morphology. For instance, during PPF, actin may play an important role in bending and branching [17]. This evidence suggests that actomyosin could play an important role in the generation of proplatelets.

In the present study, calyculin A treatment led to proplatelets retraction of mature MKs that were derived from ES cells. In the case of human platelets, calyculin A or okadaic acid induces the pseudopods [18], as well as slow MLC phosphorylation [19]. The circumferential microtubule bands become disrupted, and many short microtubule fragments become randomly dispersed throughout the platelet

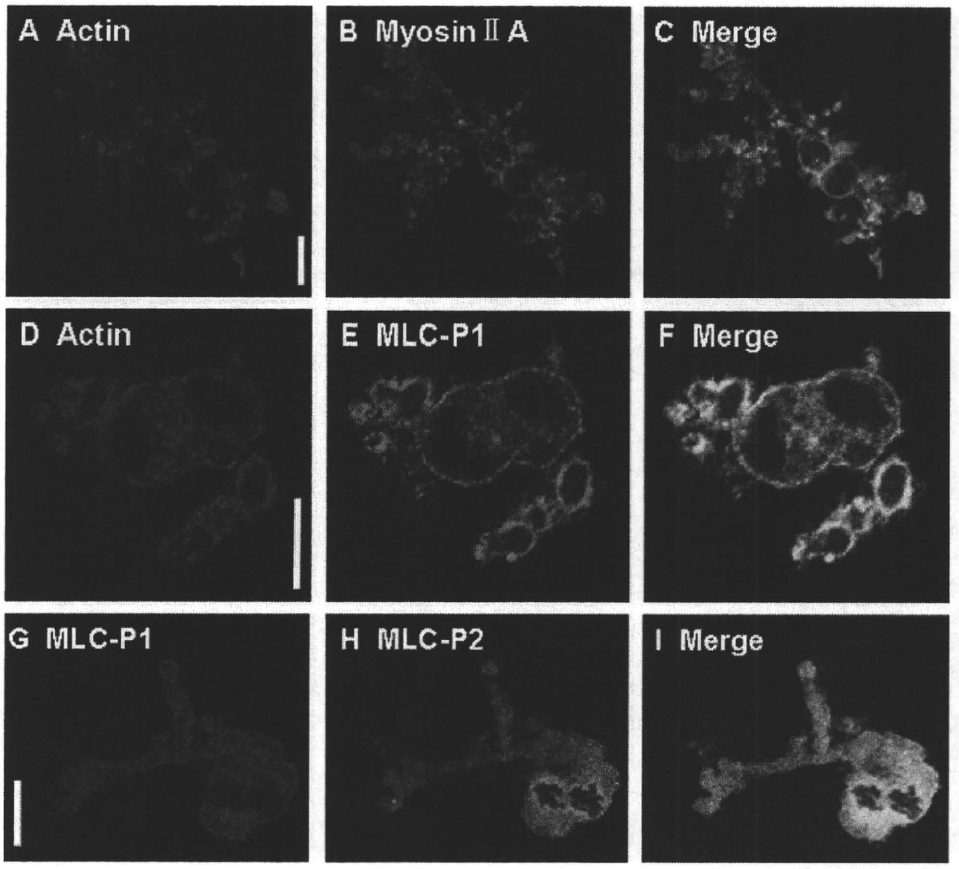

Fig. 3. Localization of actin, myosin IIA, MLC-P1, and MLC-P2 of calyculin A-treated PPF. MK proplatelets were stimulated with 50 nM calyculin A. After 5 min, cells were fixed, permeabilized, and incubated with respective antibodies. (A) Actin (red), (B) myosin IIA (green), (C) merge of actin (A), and myosin IIA (B). (D) Actin (red), (E) MLC-P1 (green), (F) merge of actin (D), and MLC-P1(E). (G) MLC-P1 (red), (H) MLC-P2 (green), (I) merge of MLC-P1 (G), and MLC-P2 (H). Cell nuclei were also stained with DAPI (blue). Scale bar, 10 μm. (For interpretation of the references to color in this figure legend, the reader is referred to the web version of this article.)

cytoplasm through calyculin A and okadaic acid treatment [8]. In addition, actin depolymerization has been observed in renal epithelial cells LLC-PK1 after calyculin A treatment [20]. These changes may also take place in retracted MK cells following calyculin A treatment (Fig. 4).

The effects of various agents on the PPF of mature, ES-derived MKs were explored; forskolin, GF109203X, Y-27632, PMA, cytochalasin D, and paclitaxel were tested *in vitro*. Forskolin is one of the compounds that elevate cellular cyclic AMP and stimulate MKs to undergo PPF in a dose-dependent manner [21]. GF109203X is a PKC inhibitor, and Y-27632 is a Rho-kinase inhibitor; both inhibit thrombin-induced morphological changes in the megakaryocytic leukemia cell line UT-7/TPO [12]. Inhibition of PKC results in a reduction murine MKs undergoing PPF [16]; however, Y-27632 promotes MKs derived from human $CD34^+$ cells to commence PPF [22]. PMA has been shown to induce differentiation in megakaryocytic cells, e.g., K562 cells and Dami cells.

Tablin et al. demonstrated that proplatelet elongation is dependent on microtubules [23]. Paclitaxel, which stabilizes microtubules, is able to completely block bending and branching along the length of the proplatelet tube and increase both the diameter of individual tubes and the thickness of microtubule bundles within them [17]. When MKs were cultured in the presence of cytochalasin B or cytochalasin D, which are inhibitors of actin assembly, the cells retained the capacity to extend long, slender proplatelet-like projections, along with other abnormal features [17]. These agents were all tested to determine whether they were able to influence PPF; however, only calyculin A could alter the PPF of MKs.

We previously reported thrombin-induced morphological changes in the TPO-dependent human megakaryocytic cell line UT-7/TPO [12]. In unstimulated cells, MLC-P1 was distributed throughout the cytoplasm, whereas MLC-P2 was localized to the cortical region [12]. Sixty seconds after thrombin stimulation, MLC-P2 continued to be expressed in the cortical region, as well as MLC-P1 [12]. In the present study, although MLC-P1 and MLC-P2 were diffusely expressed in the PPF of untreated MKs, the redistribution of MLC-P1 and MLC-P2 was observed in calyculin A-treated cells. This suggests that MLC-P2 was present in the area that required influences such as proplatelet retraction.

In conclusion, we demonstrated that calyculin A treatment results in proplatelet retraction of ES-derived MK cells. Protracted MLC phosphorylation, actin depolymerization, and microtubule disruption could all be factors

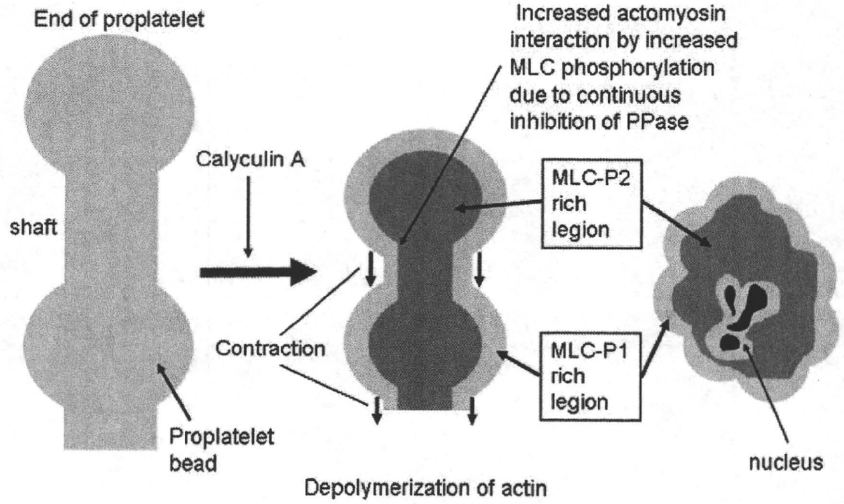

Fig. 4. Hypothetical mechanism of calyculin A-induced retraction of mature MK proplatelets. Actomyosin interaction was induced by MLC phosphorylation due to continuous inhibition of protein phosphatase by calyculin A treatment. MLC-P1 was expressed strongly in the cortical region, and MLC-P2 expression primarily surrounded the nucleus and the inner area of proplatelets. Concurrently, calyculin A treatment resulted in actin depolymerization. The induction of proplatelet retraction could be induced by each of these factors. PPase, protein phosphatase.

stimulating this retraction (Fig. 4). We propose that the maintenance of actomyosin force is controlled by MLC phosphorylation during PPF.

References

[1] Y. Chang, D. Bluteau, N. Debili, W. Vainchenker, From hematopoietic stem cells to platelets, J. Thromb. Haemost. 5 (Suppl. 1) (2007) 318–327.

[2] T. Nakano, H. Kodama, T. Honjo, Generation of lymphohematopoietic cells from embryonic stem cells in culture, Science 265 (1994) 1098–1101.

[3] T. Nakano, H. Kodama, T. Honjo, In vitro development of primitive and definitive erythrocytes from different precursors, Science 272 (1996) 722–724.

[4] T.T. Fujimoto, S. Kohata, H. Suzuki, H. Miyazaki, K. Fujimura, Production of functional platelets by differentiated embryonic stem (ES) cells in vitro, Blood 102 (2003) 4044–4051.

[5] K. Murata, M. Sakon, J. Kambayashi, M. Yukawa, H. Ariyoshi, E. Shiba, T. Kawasaki, J. Kang, T. Mori, The effects of okadaic acid and calyculin A on thrombin induced platelet reaction, Biochem. Int. 26 (1992) 327–334.

[6] M. Nishikawa, H. Toyoda, M. Saito, K. Morita, I. Tawara, K. Deguchi, T. Kuno, H. Shima, M. Nagao, S. Shirakawa, Calyculin A and okadiac acid inhibit human platelet aggregation by blocking protein phosphatases types 1 and 2A, Cell Signal. 6 (1994) 59–71.

[7] Y. Yano, J. Kambayashi, E. Shiba, M. Sakon, E. Oiki, K. Fukuda, T. Kawasaki, T. Mori, The role of protein phosphorylation and cytoskeletal reorganization in microparticle formation from the platelet plasma membrane, Biochem. J. 299 (1994) 303–308.

[8] Y. Yano, M. Sakon, J. Kambayashi, T. Kawasaki, T. Senda, K. Tanaka, F. Yamada, N. Shibata, Cytoskeletal reorganization of human platelets induced by the protein phosphatase 1/2 A inhibitors okadaic acid and calyculin A, Biochem. J. 307 (1995) 439–449.

[9] K. Itoh, T. Hara, F. Yamada, N. Shibata, Diphosphorylation of platelet myosin ex vivo in the initial phase of activation by thrombin, Biochim. Biophys. Acta 1136 (1992) 52–56.

[10] M. Ikebe, D.J. Hartshorne, Phosphorylation of smooth muscle myosin at two distinct sites by myosin light chain kinase, J. Biol. Chem. 260 (1985) 10027–10031.

[11] M. Ikebe, Phosphorylation of a second site for myosin light chain kinase on platelet myosin, Biochemistry 28 (1989) 8750–8755.

[12] A. Yazaki, S. Tamaru, Y. Sasaki, N. Komatsu, H. Wada, H. Shiku, M. Nishikawa, Inhibition by Rho-kinase and protein kinase C of myosin phosphatase is involved in thrombin-induced shape change of megakaryocytic leukemia cell line UT-7/TPO, Cell Signal. 17 (2005) 321–330.

[13] M. Uehata, T. Ishizaki, H. Satoh, T. Ono, T. Kawahara, T. Morishita, H. Tamakawa, K. Yamagami, J. Inui, M. Maekawa, S. Narumiya, Calcium sensitization of smooth muscle mediated by a Rho-associated protein kinase in hypertension, Nature 389 (1997) 990–994.

[14] D. Toullec, P. Pianetti, H. Coste, P. Bellevergue, T. Grand-Perret, M. Ajakane, V. Baudet, P. Boissin, E. Boursier, F. Loriolle, et al., The bisindolylmaleimide GF 109203X is a potent and selective inhibitor of protein kinase C, J. Biol. Chem. 266 (1991) 15771–15781.

[15] K. Sakurada, M. Seto, Y. Sasaki, Dynamics of myosin light chain phosphorylation at Ser19 and Thr18/Ser19 in smooth muscle cells in culture, Am. J. Physiol. 274 (1998) C1563–C1572.

[16] P. Rojnuckarin, K. Kaushansky, Actin reorganization and proplatelet formation in murine megakaryocytes: the role of protein kinase calpha, Blood 97 (2001) 154–161.

[17] J.E. Italiano Jr., P. Lecine, R.A. Shivdasani, J.H. Hartwig, Blood platelets are assembled principally at the ends of proplatelet processes produced by differentiated megakaryocytes, J. Cell. Biol. 147 (1999) 1299–1312.

[18] H. Kawakami, M. Higashihara, X.H. Song, K. Kurokawa, M. Ikebe, H. Hirano, Okadaic acid induces marked shape change of human platelets, J. Smooth Muscle Res. 30 (1994) 57–64.

[19] F. Stark, R. Golla, V.T. Nachmias, Formation and contraction of a microfilamentous shell in saponin-permeabilized platelets, J. Cell. Biol. 112 (1991) 903–913.

[20] L. Gu, H. Zhang, Q. Chen, J. Chen, Calyculin A-induced actin phosphorylation and depolymerization in renal epithelial cells, Cell Motil. Cytoskeleton 54 (2003) 286–295.

[21] R.M. Leven, Differential regulation of integrin-mediated proplatelet formation and megakaryocyte spreading, J. Cell. Physiol. 163 (1995) 597–607.

[22] Y. Chang, F. Aurade, F. Larbret, Y. Zhang, J.P. Le Couedic, L. Momeux, J. Larghero, J. Bertoglio, F. Louache, E. Cramer, W. Vainchenker, N. Debili, Proplatelet formation is regulated by the Rho/ROCK pathway, Blood 109 (2007) 4229–4236.

[23] F. Tablin, M. Castro, R.M. Leven, Blood platelet formation in vitro. The role of the cytoskeleton in megakaryocyte fragmentation, J. Cell. Sci. 97 (1990) 59–70.

Pivotal Role of Lnk Adaptor Protein in Endothelial Progenitor Cell Biology for Vascular Regeneration

Sang-Mo Kwon,* Takahiro Suzuki,* Atsuhiko Kawamoto, Masaaki Ii, Masamichi Eguchi, Hiroshi Akimaru, Mika Wada, Tomoyuki Matsumoto, Haruchika Masuda, Yoshihiro Nakagawa, Hiromi Nishimura, Kenji Kawai, Satoshi Takaki, Takayuki Asahara

Abstract—Despite the fact that endothelial progenitor cells (EPCs) are important for postnatal neovascularization, their origins, differentiation, and modulators are not clear. Here, we demonstrate that Lnk, a negative regulator of hematopoietic stem cell proliferation, controls endothelial commitment of c-kit$^+$/Sca-1$^+$/Lineage$^-$ (KSL) subpopulations of bone marrow cells. The results of EPC colony–forming assays reveal that small (primitive) EPC colony formation by CD34$^-$ KSLs and large (definitive) EPC colony formation by CD34$^{(dim)}$ KSLs are more robust in *lnk*$^{-/-}$ mice. In hindlimb ischemia, perfusion recovery is augmented in *lnk*$^{-/-}$ mice through enhanced proliferation and mobilization of EPCs via c-Kit/stem cell factor. We found that Lnk-deficient EPCs are more potent actors than resident cells in hindlimb perfusion recovery and ischemic neovascularization, mainly via the activity of bone marrow-EPCs. Similarly, *lnk*$^{-/-}$ mice show augmented retinal neovascularization and astrocyte network maturation without an increase in indicators of pathogenic angiogenesis in an in vivo model of retinopathy. Taken together, our results provide strong evidence that Lnk regulates bone marrow-EPC kinetics in vascular regeneration. Selective targeting of Lnk may be a safe and effective strategy to augment therapeutic neovascularization by EPC transplantation. (*Circ Res.* 2009;104:969-977.)

Key Words: endothelial progenitor cell ■ lnk ■ vascular regeneration

Stem cell–related, postnatal neovascularization requires several activities of putative stem cells and their progeny, endothelial progenitor cells (EPCs), including the ability to self-renew in bone marrow (BM), commitment and differentiation into mature endothelial cells (ECs), mobilization from BM into the circulatory system, and recruitment to sites of neovascularization.[1,2] Many cytokines augment mobilization and/or recruitment of BM-derived EPCs,[3,4] including granulocyte colony-stimulating factor and granulocyte/macrophage colony-stimulating factor; angiogenic growth factors such as vascular endothelial growth factor (VEGF) and stromal cell–derived factor (SDF)-1; estrogen; and pharmaceutical drugs such as statins. However, these factors act not only on immature stem/progenitor cells but also on hematopoietic cells and mature ECs. Thus, the identification of a novel molecule that specifically regulates immature populations involved in EPC kinetics in BM is warranted.

Differentiation of progenitor cells into hematopoietic and endothelial lineage cells has been intensively investigated. During development, hemangioblastic aggregates originate from the mesodermal yolk sac, migrate to the fetal liver, and finally establish themselves in the BM. The results of a number of gene-targeting studies contribute to our understanding of functional molecules such as Scl/Tal,[5] c-kit, CD34, Runx-1,[6] and Flk-1,[7] which regulate the developmental kinetics of hemangioblasts and are also expressed in the common precursors of hematopoietic cells and ECs. Postnatal hematopoietic stem cells (HSCs) and EPCs also share common markers; however, the precise characteristics of hemangioblasts, mechanisms regulating cell growth in adults, and endothelial commitment of putative stem cells and/or common precursors for hematopoietic cells and ECs for postnatal vasculogenesis have not previously been reported.

The Lnk protein shares a pleckstrin homology domain, a Src homology 2 domain, and potential tyrosine phosphorylation sites with APS and SH-2B. It belongs to a family of adaptor proteins implicated in integration and regulation of multiple signaling events.[8] Lnk has been studied in the immune system, where Lnk regulates B cell production via negative regulation of pro–B-cell expansion.[8] Recently, Lnk was reported to play a critical role in maintaining the ability of HSCs to self-renew, in a study that based on BM c-Kit$^+$/Sca-1$^+$/Lineage (Lin)$^-$ (KSL) CD34$^-$ cells, which are

Original received December 16, 2008; revision received February 12, 2009; accepted March 17, 2009.

From the Departments of Regenerative Medicine Science (S.-M.K., M.E., M.W., H.M., K.K., T.A.) and Ophthalmology (T.S., Y.N.), Tokai University School of Medicine, Isehara; Vascular Regeneration Research Group (S.-M.K., A.K., M.I., H.A., T.M., H.N., T.A.), Institute of Biomedical Research and Innovation, Kobe; and Department of Community Health and Medicine (S.T.), Research Institute, International Medical Center of Japan, Tokyo.

*Both authors contributed equally to this work.

Correspondence to Takayuki Asahara, MD, PhD, Department of Regenerative Medicine Science, Tokai University School of Medicine, 143 Shimokasuya, Isehara, Kanagawa, Japan 259-1193. E-mail asa777@is.icc.u-tokai.ac.jp

Circulation Research is available at http://circres.ahajournals.org DOI: 10.1161/CIRCRESAHA.108.192856

a more immature HSC subpopulation than KSL CD34$^+$ cells.[9] Importantly, earlier studies report that expression of *lnk* is strong in immature cells, ie, c-kit$^+$/Lin$^-$ cells, as compared with relatively mature cells, ie, c-Kit$^-$/Lin$^-$ cells.[10] Accordingly, and because mouse BM-KSLs are capable of differentiating into both hematopoietic and endothelial lineage cells and contribute to postnatal vasculogenesis,[11–13] Lnk may regulate the functional kinetics of EPCs. Lnk has also been suggested to act as a negative regulator of the stem cell factor (SCF)–c-Kit signaling pathway.[10] SCF reportedly stimulates proliferation and differentiation of HSCs and mobilizes stem cell populations from BM into peripheral blood (PB) by binding with its receptor, c-Kit. The SCF–c-Kit signaling pathway also supports stem cell survival and motility.[14] Moreover, EPCs are recruited via interaction with membrane-bound c-Kit, which is highly expressed on ECs in ischemic tissue.[15] The c-Kit–positive cells recruited to ischemic tissue reconstitute the injured heart and vasculature, via to their ability to regulate the myocardial balance of angiogenic cytokines.[16]

Here, we sought to test the hypothesis that a lack of Lnk signaling may enhance postnatal neovascularization via specific control of the SCF–c-Kit–mediated regenerative potential of EPCs. We provide in vitro and in vivo evidence that Lnk plays a pivotal role in specific modulation of EPCs in terms of cell growth, commitment into endothelial lineage cell types, mobilization from BM into PB, and recruitment to ischemic sites for neovascularization.

Materials and Methods

An expanded Materials and Methods section is available in the online data supplement at http://circres.ahajournals.org.

Mice

The *lnk*$^{-/-}$ mice were generated as previously reported.[8] All animal care and experiments were conducted in accordance with the institutional guidelines of Tokai University School of Medicine, Isehara, Japan.

EPC Kinetics

EPC colony–forming assay (EPC-CFA), single cell–based EPC-CFA, mobilization of EPCs, and in vitro 5′-bromodeoxyuridine (BrdUrd) proliferation assay were performed.

In Vivo Study

Hindlimb Ischemia Model and Cell Transplantation

The mouse model of hindlimb ischemia was generated by ligating the proximal femoral artery of 8- to 10-week-old C57BL6/J or Balb/C nude mice.

BM Transplantation Model

C57BL/6J mice were exposed to a lethal dose of total body irradiation (10 Gy) and inoculated intravenously with 1×10^6 donor BM mononuclear cells (BM-MNCs).

Murine Model of Oxygen-Induced Retinopathy

Oxygen-induced retinopathy (OIR) was induced in C57/BL6 wild-type (WT) and lnk$^{-/-}$ mice.

Results

Deficiency of *lnk* Augments Endothelial Differentiation and Upregulates Cell Growth-Relating Signals in BM-KSL Subpopulations

Although a previous report has clearly shown that self-renewal of BM-CD34$^-$ KSLs for hematopoiesis is accelerated in *lnk*$^{-/-}$ mice,[9] the role of Lnk in ischemic vasculogenesis is unknown. We first examined *lnk* mRNA levels in various populations of BM cells and several organs of WT mice in the presence or absence of limb ischemia. Expression of *lnk* mRNA is strong in BM-CD34$^-$ KSLs regardless of tissue ischemia. Expression of *lnk* is moderate in BM-CD34$^+$ KSLs, a relatively differentiated population as compared with CD34$^-$ KSLs. In contrast, *lnk* expression was faint in samples from BM-MNCs, BM-Lin$^-$ cells, skeletal muscle, and spleen independently of ischemia. These results suggest that *lnk* is highly expressed in BM hematopoietic and endothelial progenitors but not in mature BM cells or other organs. The *lnk* expression levels were especially high in the immature fraction of BM-HSC/EPCs as compared to committing fractions (Figure 1a).

The pattern of expression of *lnk* suggests a role in differentiation of various subpopulations among BM-KSLs. To test this, we next compared the number of BM-KSLs and derivative subpopulations in *lnk*$^{-/-}$ and WT mice. The number of KSLs, CD34$^-$ KSLs, and CD34$^{(dim)}$ KSLs, but not CD34$^{(high)}$ KSLs, was significantly greater in *lnk*$^{-/-}$ mice than in WT. These data suggest that deletion of *lnk* results in an increase in immature subpopulations of KSLs (Figure 1b). To compare the vasculogenic commitment of BM-KSLs in *lnk*$^{-/-}$ mice versus WT, fluorescence-activated cell-sorting analysis for endothelial markers was performed. KSLs coexpressing Flk-1 or CXCR4 were more frequent in *lnk*$^{-/-}$ mice than in WT (Figure 1c). Thus, loss of *lnk* appears to promote vasculogenic commitment, resulting in an increase in the EPC pool in BM. Similarly, the number of EPCs increased in PB of Lnk-deficient mice (Figures I and II in the online data supplement).

To further confirm the role of Lnk in differentiation of KSL subpopulations into endothelial lineage cells, we performed an EPC-CFA established recently in our laboratory. KSLs and their subpopulations can form 2 types of EPC colony clusters, small (primitive) and large (definitive) EPC colony clusters. Both cluster types are positive for uptake of acetyl LDL (Ac-LDL) and for expression of an EC-specific marker, isolectin B4, as revealed by chemical staining. Additionally, both are positive for Flk-1 (VEGF receptor 2) and CD31 (platelet endothelial cell adhesion molecule-1), as revealed by immunocytochemistry (Online Figure III, a through d). Moreover, colony-derived cells express the endothelial markers Flk-1 and CD31 at high levels, as detected by flow cytometric analysis. Cells from large EPC clusters, which comprise more committed EPCs with spindle-like morphology, more frequently show Ac-LDL uptake and higher expression of Flk-1 and CD31 than cells from small EPC clusters (Online Figure III, c and d).

EPC-CFA was performed for each KSL subpopulation obtained from *lnk*$^{-/-}$ or WT mice. The number of small EPC colonies derived from CD34$^-$ KSLs was significantly greater in *lnk*$^{-/-}$ mice than in WT, whereas the number derived from CD34$^{(dim)}$ or CD34$^{(high)}$ KSLs was similar in *lnk*$^{-/-}$ and WT. In contrast, the number of large EPC colonies from CD34$^-$ KSLs was similar in both groups, whereas the number from CD34$^{(dim)}$ or CD34$^{(high)}$ KSLs was significantly higher in *lnk*$^{-/-}$ mice than WT (Figure 1d). These data suggest that Lnk deficiency increases the capacity of immature stem cells

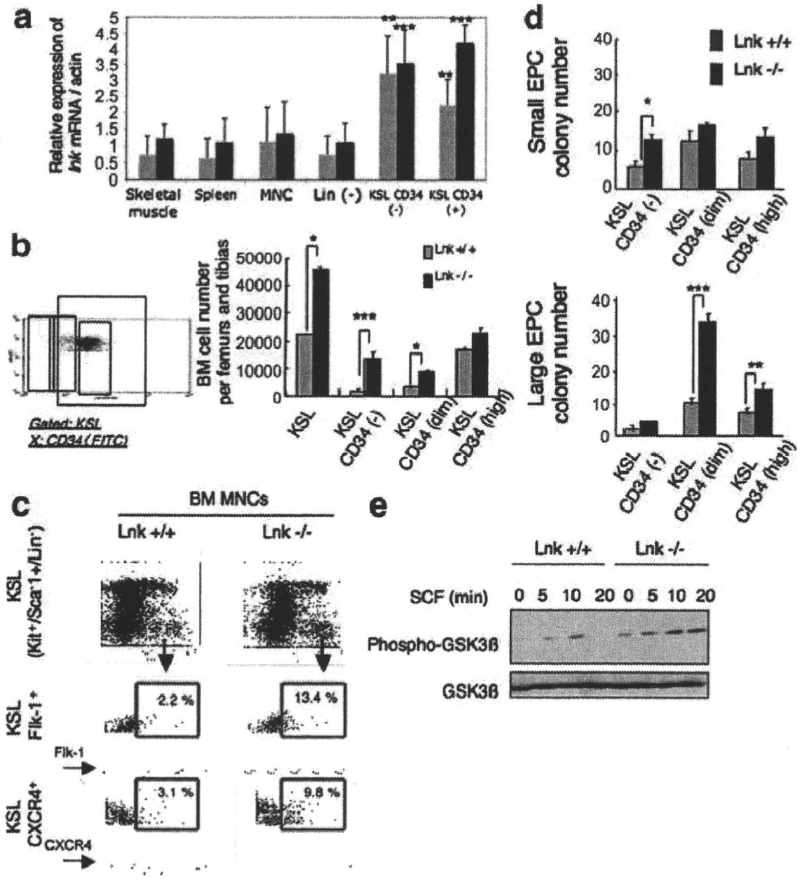

Figure 1. Lnk is pivotal for vascularization in response to ischemia. a, Relative changes in expression of *lnk* mRNA in response to ischemia. RT-PCR analysis was performed on skeletal muscle, spleen, BM-MNCs, BM-Lin$^-$ cells, and KSL subpopulations of WT mice preischemia and 3 days after hindlimb ischemia. b, Total number of KSL subpopulations by flow cytometric analysis in Lnk$^{-/-}$ mice and WT mice (n=6). c, FACS analysis of BM-KSL cells from *lnk* $^{-/-}$ and WT mice. d, EPC-CFA to evaluate vascular regeneration capacity of BM-KSL subpopulations in Lnk-deficient and WT mice. Colony number was counted 10 to 12 days after incubation of 500 cells per dish (n=4). e, Phosphorylation of GSK3β on stimulation of 100 ng/mL SCF in CD34$^{(neg)/(dim)}$ KSLs of *lnk*$^{-/-}$ and WT mice. *P<0.05, **P<0.01, ***P<0.001.

to form primitive EPCs and in the capacity of relatively mature progenitor cells to differentiate into definitive EPCs.

To compare cell growth of CD34$^-$/CD34$^{(dim)}$ KSLs from *lnk*$^{-/-}$ versus WT mice, we next analyzed SCF-dependent glycogen synthase kinase (GSK)3β phosphorylation, which is part of a signaling cascade indispensable for cell growth.[17] The level of phosphorylation of GSK3β in CD34$^-$/CD34$^{(dim)}$ KSLs was enhanced and prolonged in the *lnk*$^{-/-}$ background relative to WT. This points to an important role for Lnk in the ability of immature HSC/EPCs to cell growth, as apparently controlled by upregulation of the SCF-dependent GSK3β signaling pathway (Figure 1e).

Lnk Deficiency Upregulates Proliferation and Endothelial Commitment of EPCs Derived From KSL Populations in Culture

To explore the function of Lnk in EPC biology in terms of cell proliferation and commitment, we isolated and cultured Lin$^-$ cells, KSLs, and KSL subpopulations from WT and Lnk-deficient mice in a defined EPC culture system. In both *lnk*$^{-/-}$ and WT genetic backgrounds, KSLs in general, and CD34$^-$ KSLs and CD34$^{(dim)}$ KSLs in particular, proliferated efficiently in culture for 1 week, whereas BM-Lin$^-$ cells and CD34$^{(high)}$ KSL subpopulation cells exhibited a smaller increase in proliferation. The fold increase in cell number for KSLs, CD34$^-$ KSLs, and CD34$^{(dim)}$ KSLs was significantly greater in cells from Lnk-null mice than from WT. In contrast, the fold increase of Lin$^-$ cells and CD34$^{(high)}$ KSL subpopulation was similar in cells from *lnk*$^{-/-}$ or WT mice.

We next looked at cultured KSL subpopulations in *lnk*$^{-/-}$ and WT genetic backgrounds. The results of flow cytometric analysis reveal that cultured cells derived from CD34$^-$ KSL or CD34$^{(dim)}$ KSL subpopulations in *lnk*$^{-/-}$ mice were more frequently positive for the endothelial lineage markers Flk-1/Sca-1 and CXCR4/Sca-1 than those from WT. However, the number of cells positive for the endothelial markers among cells cultured from the CD34$^{(high)}$ KSL subpopulation was similar for *lnk*$^{-/-}$ and WT (Online Figure IV, b and c).

To determine whether EPC development from KSL subpopulations occurs at the single-cell level, we sorted single cells from each subpopulation, cultured the cells ex vivo for 1 week, and then assayed the cells using EPC-CFA and flow cytometry. EPC-CFA revealed that the number of large EPC colonies derived from a single CD34$^-$ KSL or CD34$^{(dim)}$ KSL, but not a single CD34$^{(high)}$ KSL, was significantly greater when cells were derived from *lnk*$^{-/-}$ mice. In contrast, the number of small EPC colonies derived from single cells of all subpopulations was similar in the 2 groups (Online Figure IV, d). Flow cytometry also revealed that the frequency of Sca-1$^+$/Flk-1$^+$ cells, an EPC-enriched population, among cultured cells derived from single CD34$^-$ KSLs or CD34$^{(dim)}$ KSLs, but not single CD34$^{(high)}$ KSLs, was significantly higher in *lnk*$^{-/-}$ than WT (Online Figure IV, e).

Lnk Deficiency Promotes Neovascularization In Vivo

The in vitro data above suggest that negative modulation of *lnk* gene expression may promote neovascularization in ischemic tissue. To test the in vivo effect of *lnk* deficiency,

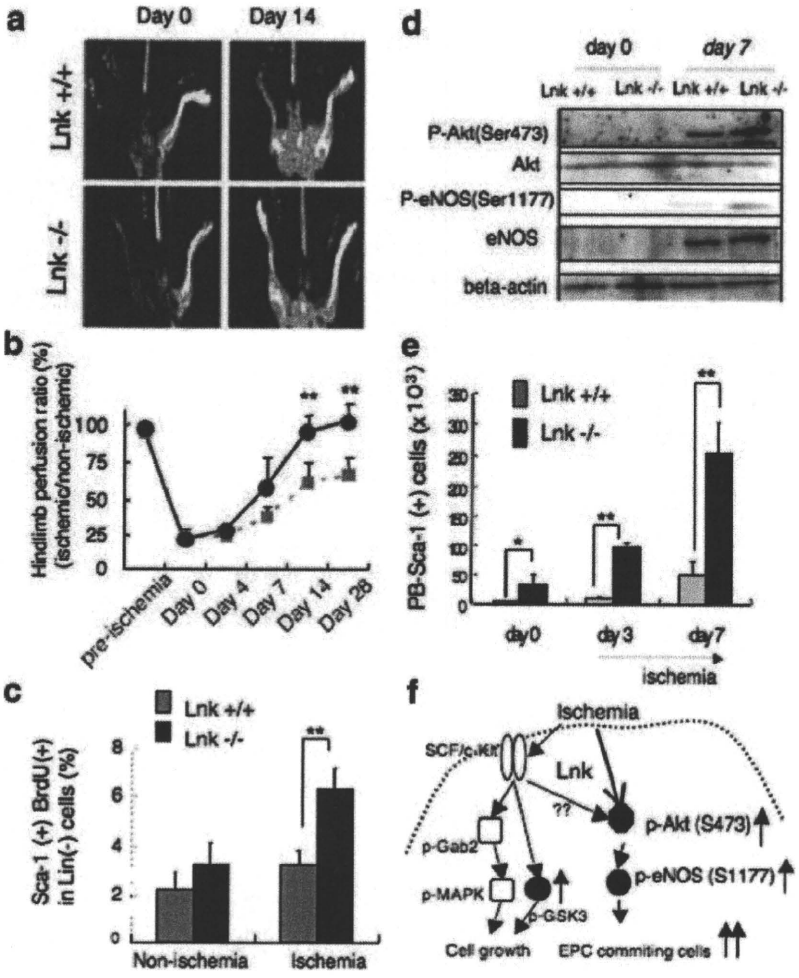

Figure 2. Neovascularization and EPC kinetics in response to hindlimb ischemia. a and b, Laser Doppler perfusion imaging (LDPI) to elucidate recovery of blood flow after ischemia in $Lnk^{-/-}$ mice and WT, expressed as the ratio of perfusion in ischemic limb to that in contralateral (nonischemic) limb (hindlimb perfusion ratio). Representative LDPI imaging (a) and serial change in hindlimb perfusion ratio (b) are shown for both groups (n=7). c, In vivo EPC proliferation activity in response to ischemia. BrdUrd incorporation into BM-derived EPCs was evaluated preischemia and 7 days after hindlimb ischemia. Percentage of $BrdUrd^+/Sca\text{-}1^+$ cells in BM Lin^- cells is shown (n=4). d, Molecular indicators of EPC differentiation in response to ischemia. Phosphorylation of Akt and eNOS in BM $Sca\text{-}1^+/Lin^-$ cells was determined by immunoblotting. P-Akt indicates phosphorylated Akt; P-eNOS, phosphorylated eNOS. e, Serial change in the number of circulating $Sca\text{-}1^+$ cells, an EPC-enriched fraction, following hindlimb ischemia in $lnk^{-/-}$ mice and WT (n=4). f, Role of Lnk in Akt/eNOS signals or GSK signals (black circle) in response to ischemia.

we generated a hindlimb ischemia model in WT and $lnk^{-/-}$ mice. Laser Doppler perfusion imaging revealed serial recovery of blood flow in the ischemic region of both groups; however, blood flow 14 and 28 days after ischemia was significantly greater in $lnk^{-/-}$ mice than in WT (Figure 2a and 2b).

To assess the mechanism of enhanced blood flow recovery in $lnk^{-/-}$ mice, we first compared the mitotic capacity of EPC-enriched populations in the presence or absence of hindlimb ischemia in $lnk^{-/-}$ and WT genetic backgrounds. The percentage of BM $Sca\text{-}1^+/BrdUrd^+$ cells in Lin^- cells without ischemia tended to be greater in $lnk^{-/-}$ mice than in WT, but the difference was not statistically significant. In contrast, the percentage of cycling EPCs 7 days after ischemia was significantly greater in $lnk^{-/-}$ mice than in WT. These data suggest that the proliferative activity of EPCs in response to ischemia is upregulated in the absence of Lnk activity (Figure 2c). Next, we compared the enhancement of ischemia-induced phosphorylation of Akt and of endothelial nitric oxide synthase (eNOS) levels in BM-$Sca\text{-}1^+/Lin^-$ cells in $lnk^{-/-}$ mice versus WT. The results indicate that Lnk-deficient EPCs are more potent for activation of the Akt/eNOS signaling cascade, an important pathway for EPC survival and differentiation (Figure 2d and 2f).[18] To clarify the potential of EPCs in $lnk^{-/-}$ mice for ischemic neovascularization, we used RT-PCR to compare mRNA expression of angiogenic factors and their receptors in KSL subpopulations in the presence or absence of hindlimb ischemia in $lnk^{-/-}$ and WT. In $lnk^{-/-}$ mice, genes that encode angiogenic factors or their receptors, such as *vegf*, *ang-1*, *tie-1*, and *tie-2*, were highly expressed independently of ischemic condition, whereas *ang-2*, an antagonist of TIE-2 signaling, was constitutively downregulated. In contrast, most angiogenic genes, which are weakly expressed at baseline, were upregulated postischemia in WT (Online Figure V). These data suggest that Lnk regulates the production of angiogenic factors, which in turn enhances EPC proliferation, differentiation, migration, and mobilization.

As for the kinetics of PB-EPCs, the number of $Sca\text{-}1^+$ MNCs, an EPC-enriched fraction, on days 3 and 7 after hindlimb ischemia was significantly increased in $lnk^{-/-}$ mice as compared to WT (Figure 2e). Furthermore, the number of $Sca\text{-}1^+/CD31^+$ and $Sca\text{-}1^+/Flk\text{-}1^+$ cells in PB was greater in $lnk^{-/-}$ mice as compared to WT (data not shown). These outcomes suggest that the mobilization of EPCs into circulation in response to ischemia is augmented in $lnk^{-/-}$ mice compared with WT.

A caveat to the above is that enhanced neovascularization in $lnk^{-/-}$ mice could be attributable to upregulation of angiogenic effects of resident cells as well as augmentation of BM-derived EPC kinetics. To clarify the proportional contribution of these mechanisms, we performed BM transplantation (BMT) with cells from $lnk^{-/-}$ or WT, with donor cells marked with green fluorescent protein (GFP) transplanted

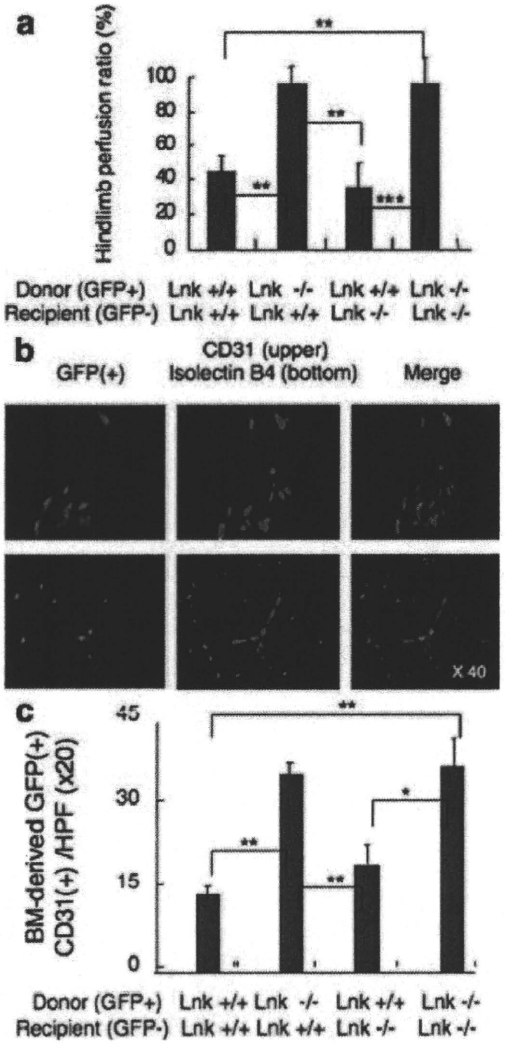

Figure 3. BM-derived EPCs predominate in blood vessel regeneration in $lnk^{-/-}$ mice. a, Ratio of donor (GFP-positive) BMTs vs host cells contributing to hindlimb perfusion 14 days after ischemia in $lnk^{-/-}$ or WT mice (n=6). b, Representative immunostaining for GFP, CD31, and isolectin B4 to identify BM-derived EPCs in ischemic tissue from WT mice perfused with BMT from $lnk^{-/-}$ mice. c, Number of BM-derived putative EPCs (ie, $GFP^+/CD31^+$ cells) in mice undergoing BMT (n=6).

into unmarked recipients. Perfusion in limb tissue at day 14 postischemia dramatically improved in WT mice that received Lnk-deficient BM cells (BMCs) as compared with WT mice receiving WT BMCs. Moreover, perfusion recovery in the hindlimb was significantly inhibited in $lnk^{-/-}$ mice receiving WT BMCs as compared with $lnk^{-/-}$ mice receiving Lnk-deficient BMCs. Importantly, hindlimb perfusion was similar in WT and $lnk^{-/-}$ mice receiving WT BMCs. Similarly, perfusion recovery was not significantly different between WT and $lnk^{-/-}$ mice receiving Lnk-deficient BMCs (Figure 3a).

Next, we detected BM-derived endothelial lineage cells incorporating into the ischemic region via immunohistochemical detection of GFP and CD31 or isolectin B4 (Figure 3b). The number of $GFP^+/CD31^+$ ECs in ischemic tissue was significantly greater in WT mice receiving Lnk-null BMCs than in those receiving WT BMCs. In addition, BM-derived ECs were more frequently observed in $lnk^{-/-}$ mice receiving Lnk-deficient BMCs than in those receiving WT BMCs. Similar to what was observed in the hindlimb perfusion analysis, the number of BM-derived ECs was equivalent in WT mice receiving Lnk-deficient BMCs and $lnk^{-/-}$ mice receiving Lnk-deficient BMCs, as well as in WT mice receiving WT BMCs and $lnk^{-/-}$ mice receiving WT BMCs (Figure 3c). These results suggest that BM-derived EPCs are indispensable for enhanced neovascularization in $lnk^{-/-}$ mice, whereas *lnk* deficiency in resident cells does not significantly contribute to ischemic neovascularization.

Lnk Deficiency Enhances EPC Kinetics in Response to Ischemia-Related Cytokines

To identify specific cytokines responsible for enhanced mobilization of BM-EPCs in $lnk^{-/-}$ mice, we investigated the effect of several potent bioactive factors on EPC mobilization in $lnk^{-/-}$ and WT genetic backgrounds. To do this, we administered G-CSF, SDF-1α, SCF, VEGF, or PBS to mice once daily over 5 days and determined the number of PB-MNCs on day 7. In both $lnk^{-/-}$ and WT mice, each factors resulted in a significant increase in the number of PB-MNCs as compared with mock treatment (PBS). The number of PB-MNCs after administration of each factor was significantly greater in $lnk^{-/-}$ mice than in WT. Notably, SCF and VEGF led to a more than 4-fold difference in PB-MNC number in $lnk^{-/-}$ versus WT (Figure 4a). The results of an EPC culture assay using PB-MNCs also revealed that the number of circulating EPCs detected after infusion of any of the factors tested significantly increased in $lnk^{-/-}$ mice as compared with WT. This difference between the 2 groups was particularly remarkable following infusion of SCF or VEGF (Figure 4b). To evaluate the scale of the Lnk-dependent SCF effect on EPC mobilization, we next looked at cell kinetics over time after SCF infusion in $lnk^{-/-}$ or WT mice. The results of serial quantification of PB-MNCs revealed a significant increase in PB-MNCs in $lnk^{-/-}$ mice that was detectable at day 2 and reached a peak on day 6 (Figure 4c). Furthermore, the results of serial FACS analysis revealed a significant increase in the PB-EPC–enriched cell fraction (ie, in $Sca\text{-}1^+/CD31^+$ or $Sca\text{-}1^+/VE\text{-}cadherin^+$ cells) that was detectable at day 0 and still observable at day 8 after initiation of SCF infusion in $lnk^{-/-}$ mice, as compared with levels in WT (Figure 4d and 4e). We next performed an in vitro proliferation assay to ask whether SCF upregulates proliferative activity of EPCs in $lnk^{-/-}$ mice as well as mobilization. In WT mice, SCF did not affect the mitotic activity of $Sca\text{-}1^+/Lin^-$ cells. In contrast, treatment with 10 ng/mL of SCF significantly augments proliferation of EPC-enriched fraction cells in $lnk^{-/-}$ mice (Figure 4f). Taken together, these data suggest that ischemia-related cytokines, in particular SCF/c-kit, are critical for both proliferation and mobilization of EPCs in $lnk^{-/-}$ mice.

Lnk-Deficient EPCs Rescue Hindlimb Ischemia Following Therapeutic Administration

To evaluate the therapeutic potential of *lnk* gene–modified EPCs in ischemic neovascularization, we isolated and intravenously transplanted BM $Sca\text{-}1^+/Lin^-$ cells from $lnk^{-/-}$ or WT mice into nude mice with hindlimb ischemia. As shown

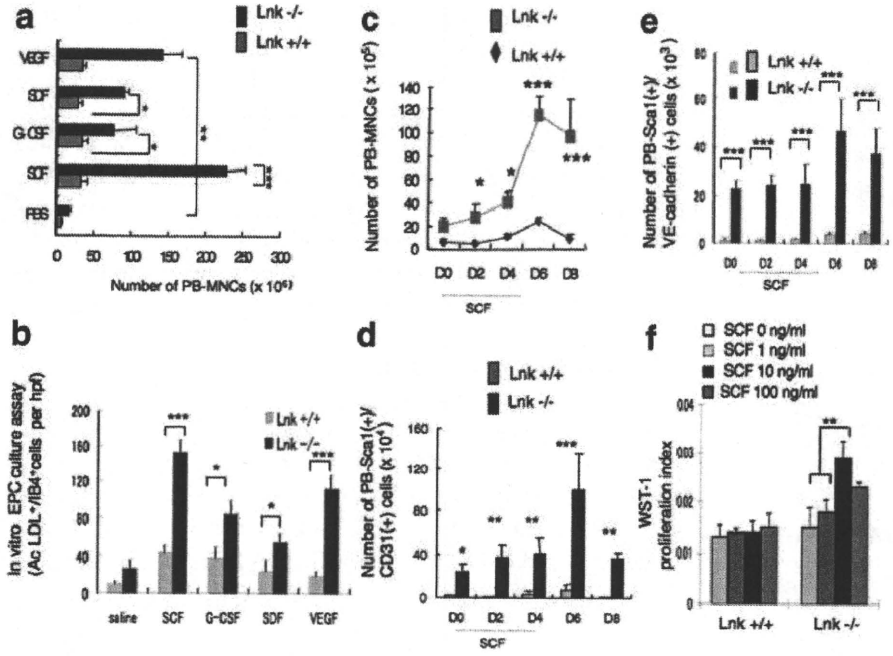

Figure 4. Effects of ischemia/angiogenesis-related cytokines on EPC kinetics are more robust in *lnk*$^{-/-}$ mice. a, Number of PB-MNCs at day 6 after initiation of VEGF, SDF-1, GCSF, SCF, or PBS in *lnk*$^{-/-}$ mice and WT (n=5). b, In vitro EPC culture assay at day 6 after initiation of VEGF, SDF-1, GCSF, SCF, or PBS in *lnk*$^{-/-}$ mice and WT (n=4). The numbers of EPCs capable of Ac-LDL uptake and positive for isolectin B4 were significantly higher in *lnk*$^{-/-}$ mice than WT. c and d, Time course of SCF-dependent mobilization kinetics in *lnk*$^{-/-}$ and WT mice (n=4 at each time point in each group). Number of circulating MNCs (c) and PB Sca-1$^+$/CD31$^+$ cells (d) was serially evaluated in both groups. e, Number of Sca-1$^+$/VE-cadherin$^+$ cells in response to SCF administration at each time calculated with the flow cytometric data. f, In vitro WST-1 proliferation assay using BM Sca-1$^+$/Lin$^-$ cells obtained from *lnk*$^{-/-}$ and WT mice in the presence of 0, 1, 10, or 100 ng/mL of SCF. $^*P<0.05$, $^{**}P<0.01$, $^{***}P<0.001$.

in Figure 5a and 5b, transplantation of Lnk-null EPCs resulted in robust hindlimb perfusion as compared with WT-EPCs at equal dosing. The results of immunohistochemical analysis using the EC markers isolectin B4 and CD31 surface antigen clearly show that the capillary density at ischemic tissues is higher in animals receiving Lnk-deficient EPCs than in those receiving WT-EPCs or a mock treatment (PBS) control (Figure 5c and 5d and Online Figure VI).

Lnk Deficiency Enhances Neonatal Revascularization in OIR

We next sought to test the effect of Lnk on vascular regeneration in retinal vascular disease. To do this, we generated an animal model of neonatal retinopathy, OIR, by exposing *lnk*$^{-/-}$ or WT mice to 75% oxygen from postnatal day (P)7 to P12 (Figure 6a). In WT mice with OIR, avascular regions of the retina were readily apparent at neonatal P17. In contrast, *lnk*$^{-/-}$ mice with OIR had 4-fold smaller retinal avascular areas than WT (Figure 6b and 6c). We also observed functional regeneration of the astrocyte network, accompanied by upregulation of blood vessel regeneration, in *lnk*$^{-/-}$ mice (Online Figure VII), suggesting that enhanced neovascularization may contribute to preservation of retinal interstitial structure in the Lnk-deficient microenvironment.

Previous results suggest that enhanced angiogenesis/vasculogenesis in the retina may result in pathogenic side effects such as excess inflammation and abnormal blood vessel formation, eventually leading to retinal bleeding.[19] However,

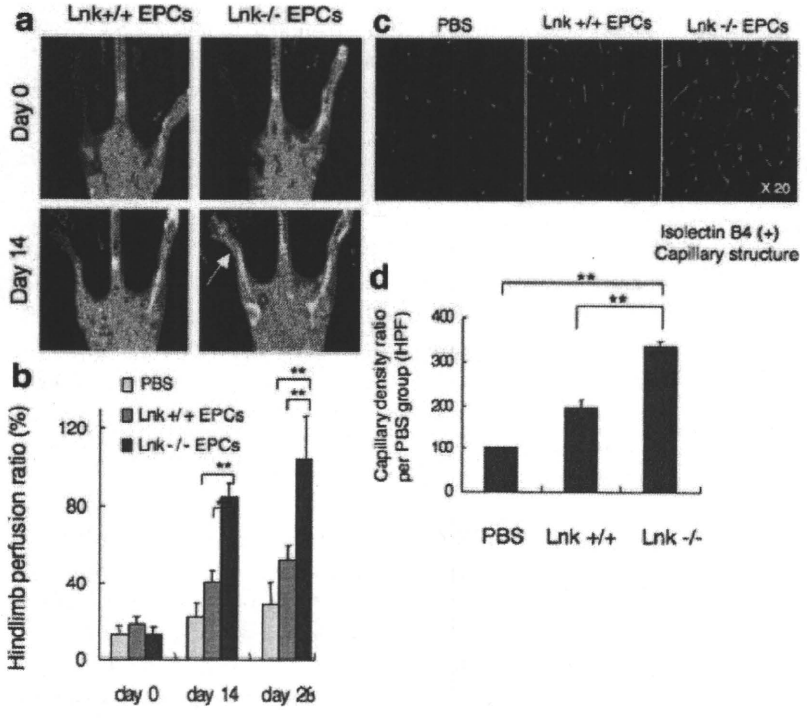

Figure 5. Lnk-deficient EPCs potently induce therapeutic neovascularization. a, Representative LDPI imaging in nude mice with hindlimb ischemia receiving BM Sca-1$^+$/Lin$^-$ cells from *lnk*$^{-/-}$ or WT mice. Arrows indicate recovery of hindlimb perfusion following Lnk-deficient EPC infusion. b, Time course of hindlimb perfusion recovery in nude mice receiving mock treatment (PBS), WT-EPCs, or *lnk*$^{-/-}$ EPCs (n=7). c, Representative capillary structure revealed by chemical staining for isolectin B4 in nude mice receiving mock treatment, WT-EPCs, or *lnk*$^{-/-}$ EPCs. d, Capillary density at day 14 after hindlimb ischemia (n=7).

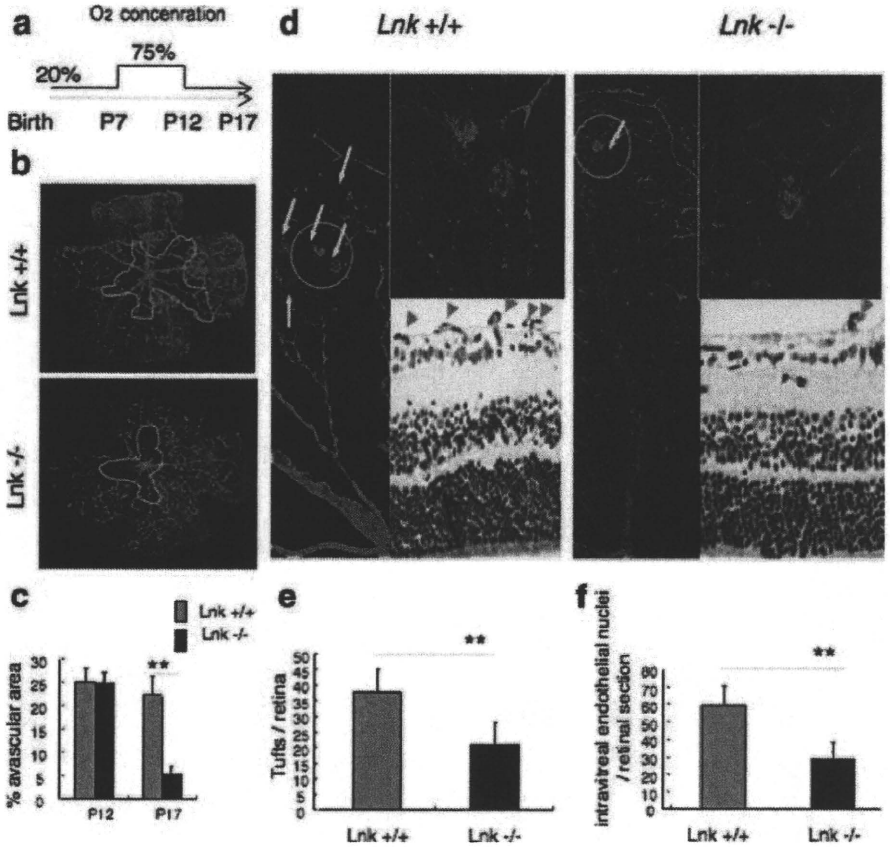

Figure 6. Augmentation of retinal neovascularization without pathogenic angiogenesis in *lnk*$^{-/-}$ mice. a, The OIR model. b, Representative immunostaining for CD31 (red) to visualize the vascular network in whole mount retina at P17 in *lnk*$^{-/-}$ and WT mice. Yellow line indicates the avascular lesion induced by hyperoxic stress. c, Percentage avascular area at P12 and P17 in *lnk*$^{-/-}$ and WT mice. d, Large images: immunostaining for CD31 (red) in P17 retinas of *lnk*$^{-/-}$ and WT mice. Arrows are tufts indicating pathogenic angiogenesis. Small images: hematoxylin/eosin staining at P17 in each group. Arrowheads indicate pathogenically formed blood vessels. e, Number of tufts per retina at P17 (n=8). f, Number of intravitreal vascular cell nuclei at P17 (n=8).

histological examination of our treated OIR model tissue revealed a smaller number of abnormally sprouting vessels in *lnk*$^{-/-}$ mice than in WT (Figure 6d through 6f). Moreover, the incidence of retinal hemorrhage at P17 was markedly lower in *lnk*$^{-/-}$ mice than in WT (Online Figures VIII and IX). These results suggest that *lnk* deficiency leads to an accelerated rate of retinal neovascularization without stimulating pathogenic blood vessel formation. To investigate this further, we isolated tissue from *lnk* deficient mice with OIR and used laser microdissection to look at the production of angiogenic growth factors in situ. Levels of VEGF, angiopoietin-1, eNOS, and leukemia inhibitory factor in vascular plexuses were significantly higher in *lnk*$^{-/-}$ mice than in WT (Figure 7b). Importantly, enhanced expression of *ang-1* may inhibit pathogenic angiogenesis by inducing the maturation of newly formed blood vessels.[20] The source of angiogenic cytokines in Lnk-null OIR is likely to be at least in part BM-derived EPCs that are recruited into the retina, as both EPCs cultured in vitro under hypoxic conditions (Online Figure X).

Discussion

The results of previous studies[12,21,22] have clearly demonstrated that BM-derived hematopoietic stem cells such as BM-KSLs serve as a reservoir of EPC origin cells in adults. In addition to having a long-term capacity for multilineage hematopoiesis, transplanted KSLs have also been shown to give rise to functional endothelial cells, even after single-cell transplantation or serial transplantation in the presence of retinal ischemic injury.[12,21] Although differentiation of hematopoietic and endothelial lineages has been intensively investigated,[5–8] molecular targets that regulate endothelial commitment of putative stem cells for postnatal vasculogenesis remain to be uncovered. Identification of molecules that control the commitment and differentiation of adult multipotent stem cells into specific lineages would be a big step toward improved therapeutic treatment in regenerative medicine. Toward identifying a modulator of endothelial development, Guthrie et al have shown that the NO pathway induces new blood vessel formation via EPCs derived from the transplanted KSLs.[22] Recently, our group reported that Jagged-1–dependent Notch signaling affects EPC bioactivities including proliferation, endothelial commitment, and mobilization from BM.[23] However, these molecules regulate multiple functions in various types of mature and immature cells. In the present study, we found a pivotal function of Lnk adaptor protein as a downstream target of the SCF–c-Kit axis that modulates vasculogenesis in BM stem cells. Lnk was most robustly expressed in BM-CD34$^-$ KSLs, which are immature putative stem cells. Lnk is also expressed at moderate levels in CD34$^+$ KSLs, a relatively differentiated stem cell type, but is not expressed in more mature cells such as BM-Lin$^-$ cells and MNCs. The results of in vitro analysis using EPC-CFA clearly indicate that Lnk deficiency results in upregulation of commitment of stem cell subpopulations into endothelial lineage cell types. Indeed, *lnk* deficiency enhances commitment of CD34$^-$ KSLs into primitive EPCs (ie, small EPC colonies). Interestingly, *lnk* deficiency also augments the activity of CD34$^{(dim)/(high)}$ KSLs for the formation of definitive EPCs (large EPC colonies). These findings suggest that Lnk may regulate not only lineage commitment but also differentiation and maturation of EPCs. The specific

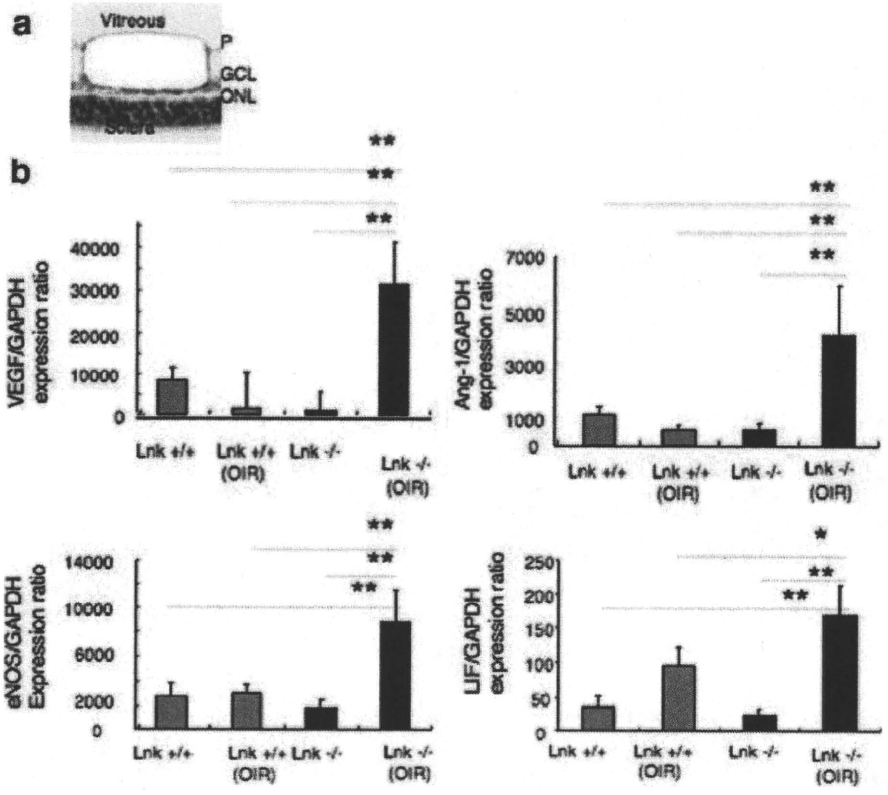

Figure 7. Augmented expression of angiogenic cytokines in *lnk*$^{-/-}$ mice. a, Representative photomicrogram showing a portion of retinal tissue dissected by laser microdissection. Counterstained with toluidine blue. P indicates periphery; GCL, ganglion cell layer; ONL, outer nuclear layer. b, Expression of angiogenic cytokines in tissue microdissected from the retina at P17 in the presence or absence of OIR induction. Expression of VEGF, Ang-1, eNOS, and leukemia inhibitory factor (LIF) mRNA was upregulated in the *lnk*$^{-/-}$ retina following OIR relative to the other groups (n=10).

expression of Lnk in stem cells and the capacity of Lnk to control lineage commitment/differentiation of BM stem cells suggest a pivotal role for Lnk as a regulator of EPCs in adults.

In addition to suggesting roles for Lnk in EPC commitment and differentiation, the results presented here also indicate that Lnk deficiency results in higher levels of proliferation of BM-KSLs and their subpopulations in vitro. Thus, we used an animal model of hindlimb ischemia to assess the effects of Lnk deficiency on EPC kinetics in vivo. Lnk deficiency results in enhanced recovery of hindlimb perfusion via upregulated proliferation of BM-derived EPCs, their enhanced mobilization activity into PB, and markedly increased recruitment into sites of ischemia. These data strongly suggest that both production of quiescent stem cells in the BM and the supply of stem cells from the BM pool for ischemic vasculogenesis may be controlled by Lnk. Furthermore, overexpression of angiogenic cytokines in Lnk-deficient KSL subpopulations suggests the importance of paracrine effects of KSL subpopulations for in situ angiogenesis as well as their autocrine effect for direct vasculogenesis. Interestingly, the results of a series of BMT experiments show that Lnk deficiency in BM-derived EPCs, but not resident EPCs/ECs, specifically augments neovascularization post hindlimb ischemia. These results provide the first direct evidence that the Lnk adapter protein plays a pivotal role in regulating the bioactivities of BM-derived EPCs for postnatal neovascularization.

Using OIR as a model for retinal damage, we also found that signs of pathogenic angiogenesis in the retina, such as tuft formation and retinal hemorrhage, were much lower in Lnk-deficient mice than in WT. Regeneration of a mature astrocyte network, along with robust neovascularization in *lnk*$^{-/-}$ mice, further supports the idea that knockdown of Lnk can have a beneficial and nonpathogenic effect in retinal vascular disease (Figure 6a through 6h and Online Figures VIII and IX). This notion may be explained by the beneficial effects of Ang-1 stimulation of vessel maturation.[22] Consistent with this, quantitative RT-PCR using microdissected retinal tissue revealed higher levels of expression of *ang-1* and other angiogenic cytokines, VEGF and eNOS, in Lnk-null mice than in WT (Figure 7b).

In conclusion, we provide strong evidence that Lnk is a definitive regulator of BM-EPC kinetics, including the ability to cell growth, endothelial commitment, mobilization, and recruitment for vascular regeneration. Selective targeting of Lnk may be a safe and effective approach to augment therapeutic neovascularization by EPC transplantation.

Acknowledgments

We thank Rie Ito for technical assistance and Sachie Ota for administrative support. We also thank all our colleagues for their helpful advice and encouragement. We appreciate assistance from the Research Center for Regenerative Medicine, the Teaching and Research Support Center, and the animal facility in the Tokai University School of Medicine and RIKEN Center for Developmental Biology.

Sources of Funding

This work was supported by the Academic Frontier Promotion Program of the Ministry of Education, Culture, Sports, Science, and Technology in Japan and a grant from the RIKEN Center for Developmental Biology.

Disclosures

None.

References

1. Asahara T, Murohara T, Sullivan A, Silver M, van der Zee R, Li T, Witzenbichler B, Schatteman G, Isner JM. Isolation of putative progenitor endothelial cells for angiogenesis. *Science*. 1997;275:964–967.

2. Asahara T, Masuda H, Takahashi T, Kalka C, Pastore C, Silver M, Kearne M, Magner M, Isner JM. Bone marrow origin of endothelial progenitor cells responsible for postnatal vasculogenesis in physiological and pathological neovascularization. *Circ Res.* 1999;85:221–228.
3. Iwakura A, Luedemann C, Shastry S, Hanley A, Kearney M, Aikawa R, Isner JM, Asahara T, Losordo DW. Estrogen-mediated, endothelial nitric oxide synthase-dependent mobilization of bone marrow-derived endothelial progenitor cells contributes to reendothelialization after arterial injury. *Circulation.* 2003;108:3115–3121.
4. Llevadot J, Murasawa S, Kureishi Y, Uchida S, Masuda H, Kawamoto A, Walsh K, Isner JM, Asahara T. HMG-CoA reductase inhibitor mobilizes bone marrow–derived endothelial progenitor cells. *J Clin Invest.* 2001; 108:399–405.
5. Gering M, Rodaway AR, Gottgens B, Patient RK, Green AR. The SCL gene specifies haemangioblast development from early mesoderm. *EMBO J.* 1998;17:4029–4045.
6. Hirai H, Samokhvalov IM, Fujimoto T, Nishikawa S, Imanishi J, Nishikawa S. Involvement of Runx1 in the down-regulation of fetal liver kinase-1 expression during transition of endothelial cells to hematopoietic cells. *Blood.* 2005;106:1948–1955.
7. Choi K, Kennedy M, Kazarov A, Papadimitriou JC, Keller G. A common precursor for hematopoietic and endothelial cells. *Development.* 1998; 125:725–732.
8. Takaki S, Sauer K, Iritani BM, Chien S, Ebihara Y, Tsuji K, Takatsu K, Perlmutter RM. Control of B cell production by the adaptor protein lnk. Definition Of a conserved family of signal-modulating proteins. *Immunity.* 2000;13:599–609.
9. Ema H, Sudo K, Seita J, Matsubara A, Morita Y, Osawa M, Takatsu K, Takaki S, Nakauchi H. Quantification of self-renewal capacity in single hematopoietic stem cells from normal and Lnk-deficient mice. *Dev Cell.* 2005;8:907–914.
10. Takaki S, Morita H, Tezuka Y, Takatsu K. Enhanced hematopoiesis by hematopoietic progenitor cells lacking intracellular adaptor protein, Lnk. *J Exp Med.* 2002;195:151–160.
11. Bailey AS, Jiang S, Afentoulis M, Baumann CI, Schroeder DA, Olson SB, Wong MH, Fleming WH. Transplanted adult hematopoietic stems cells differentiate into functional endothelial cells. *Blood.* 2004;103: 13–19.
12. Jackson KA, Majka SM, Wang H, Pocius J, Hartley CJ, Majesky MW, Entman ML, Michael LH, Hirschi KK, Goodell MA. Regeneration of ischemic cardiac muscle and vascular endothelium by adult stem cells. *J Clin Invest.* 2001;107:1395–1402.
13. Rafii S, Lyden D. Therapeutic stem and progenitor cell transplantation for organ vascularization and regeneration. *Nat Med.* 2003;9:702–712.
14. Rafii S, Heissig B, Hattori K. Efficient mobilization and recruitment of marrow-derived endothelial and hematopoietic stem cells by adenoviral vectors expressing angiogenic factors. *Gene Ther.* 2002;9:631–641.
15. Dentelli P, Rosso A, Balsamo A, Colmenares Benedetto S, Zeoli A, Pegoraro M, Camussi G, Pegoraro L, Brizzi MF. C-KIT, by interacting with the membrane-bound ligand, recruits endothelial progenitor cells to inflamed endothelium. *Blood.* 2007;109:4264–4271.
16. Fazel S, Cimini M, Chen L, Li S, Angoulvant D, Fedak P, Verma S, Weisel RD, Keating A, Li RK. Cardioprotective c-kit+ cells are from the bone marrow and regulate the myocardial balance of angiogenic cytokines. *J Clin Invest.* 2006;116:1865–1877.
17. Trowbridge JJ, Xenocostas A, Moon RT, Bhatia M. Glycogen synthase kinase-3 is an in vivo regulator of hematopoietic stem cell repopulation. *Nat Med.* 2006;12:89–98.
18. Hiasa K, Ishibashi M, Ohtani K, Inoue S, Zhao Q, Kitamoto S, Sata M, Ichiki T, Takeshita A, Egashira K. Gene transfer of stromal cell-derived factor-1alpha enhances ischemic vasculogenesis and angiogenesis via vascular endothelial growth factor/endothelial nitric oxide synthase-related pathway: next-generation chemokine therapy for therapeutic neovascularization. *Circulation.* 2004;109:2454–2461.
19. Chen J, Somanath PR, Razorenova O, Chen WS, Hay N, Bornstein P, Byzova TV. Akt1 regulates pathological angiogenesis, vascular maturation and permeability in vivo. *Nat Med.* 2005;11:1188–1196.
20. Uemura A, Ogawa M, Hirashima M, Fujiwara T, Koyama S, Takagi H, Honda Y, Wiegand SJ, Yancopoulos GD, Nishikawa S. Recombinant angiopoietin-1 restores higher-order architecture of growing blood vessels in mice in the absence of mural cells. *J Clin Invest.* 2002;110: 1619–1628.
21. Cogle CR, Scott EW. The hemangioblast: cradle to clinic. *Exp Hematol.* 2004;32:885–890.
22. Guthrie SM, Curtis LM, Mames RN, Simon GG, Grant MB, Scott EW. The nitric oxide pathway modulates hemangioblast activity of adult hematopoietic stem cells. *Blood.* 2005;105:1916–1922.
23. Kwon SM, Eguchi M, Wada M, Iwami Y, Hozumi K, Iwaguro H, Masuda H, Kawamoto A, Asahara T. Specific Jagged-1 signal from bone marrow microenvironment is required for endothelial progenitor cell development for neovascularization. *Circulation.* 2008;118:157–165.

TGF-β as a candidate bone marrow niche signal to induce hematopoietic stem cell hibernation

Satoshi Yamazaki,[1,2] Atsushi Iwama,[3,4] Shin-ichiro Takayanagi,[1] Koji Eto,[1] Hideo Ema,[1] and Hiromitsu Nakauchi[1,5]

[1]Laboratory of Stem Cell Therapy, Center for Experimental Medicine, The Institute of Medical Science, University of Tokyo, Tokyo; [2]ReproCELL, Tokyo; [3]Department of Cellular and Molecular Medicine, Graduate School of Medicine, Chiba University, Chiba; and [4]Japan Science and Technology Agency (JST), Core Research for Evolutional Science and Technology (CREST) and [5]JST, Exploratory Research for Advanced Technology (ERATO), Sanbancho, Chiyoda-ku, Tokyo, Japan

Hematopoietic stem cells (HSCs) reside in a bone marrow niche in a nondividing state from which they occasionally are aroused to undergo cell division. Yet, the mechanism underlying this unique feature remains largely unknown. We have recently shown that freshly isolated CD34⁻KSL hematopoietic stem cells (HSCs) in a hibernation state exhibit inhibited lipid raft clustering. Lipid raft clustering induced by cytokines is essential for HSCs to augment cytokine signals to the level enough to re-enter the cell cycle. Here we screened candidate niche signals that inhibit lipid raft clustering, and identified that transforming growth factor-β (TGF-β) efficiently inhibits cytokine-mediated lipid raft clustering and induces HSC hibernation ex vivo. Smad2 and Smad3, the signaling molecules directly downstream from and activated by TGF-β receptors were specifically activated in CD34⁻KSL HSCs in a hibernation state, but not in cycling CD34⁺KSL progenitors. These data uncover a critical role for TGF-β as a candidate niche signal in the control of HSC hibernation and provide TGF-β as a novel tool for ex vivo modeling of the HSC niche. (Blood. 2009;113:1250-1256)

Introduction

Dormancy or hibernation of hematopoietic stem cells (HSCs), which is indispensable for HSC maintenance, is known to occur solely in the particular bone marrow (BM) microenvironment known as the HSC niche. Most of the HSCs are in the G_0 phase in the BM niche. However, HSCs are recruited into the cell cycle at long intervals, on average every 1 to 2 months.[1,2] Thus, the capacity to enter and to leave a hibernation-like state is one of the properties of "stemness." The so-called stromal cells in the HSC BM niche, including osteoblasts, fibroblasts, adipocytes, and endothelial cells, produce several secreted and membrane-bound growth factors.[3] Several signaling pathways have been characterized that keep HSCs in hibernation or undifferentiated states. These include the Ang-1–Tie-2 signal,[4] the Notch ligand–Notch signal,[5] the N-cadherin homotypic signal,[6] and the transforming growth factor-β (TGF-β) signal.[7] However, the precise molecular mechanisms underlying HSC hibernation remain largely elusive.

Mouse BM HSCs are enriched exclusively in CD34⁻c-Kit⁺Sca-1⁺ lineage marker–negative (Lin⁻) (CD34⁻KSL) cells, a population representing 0.004% of BM mononuclear cells, whereas CD34⁺KSL cells are progenitors with short-term repopulating capacity.[8] We have recently reported that HSCs use the PI3K-Akt-FoxO signaling pathway to regulate their hibernation state, as does *C elegans* in dauer formation.[9] Akt is inactive in the cytoplasm of freshly isolated hibernating CD34⁻KSL HSCs, and FoxOs, its downstream targets, are active in their nuclei. In contrast, Akt is active in cycling CD34⁺KSL progenitors and phosphorylated FoxOs are excluded to the cytoplasm. Of note is our discovery that lipid raft status finely tunes cytokine signal levels and regulates Akt activity. Lipid raft microdomains are cholesterol- and glycosphingolipid-enriched patches in the plasma membrane into which various functional molecules are distributed. Lipid rafts act as platforms for cellular functions that include cytokine signaling, membrane trafficking, and cytoskeleton organization.[10] Because larger rafts have greater potential for concentration of transducers and for exclusion of negative regulators, lipid raft size controls signal intensity and functional outcomes. HSCs freshly isolated from the BM niche lacked lipid raft clustering (LRC). However, cytokine-induced LRC was essential for augmentation of HSC cytokine signals to levels sufficient for cell-cycle re-entry. Conversely, inhibition of LRC in HSCs attenuated cytokine signals, leading to repression of Akt followed by sustained nuclear accumulation of FoxOs, and induced a hibernation-like state in CD34⁻KSL HSCs ex vivo.

The FoxO subfamily of transcription factors is involved in diverse physiologic processes.[11] Upon activation by growth factors, the serine/threonine kinase Akt directly phosphorylates FoxO1, FoxO3, and FoxO4, resulting in their nuclear exclusion and subsequent degradation. In the absence of growth factors or in the presence of stressful stimuli, FoxOs are translocated to the nucleus and up-regulate the expression of a series of target genes, thereby promoting cell-cycle arrest, stress resistance, or apoptosis.[12] Mice that were conditionally deleted of *FoxO1, FoxO3,* and *FoxO4* in adult hematopoietic system exhibited defective long-term repopulating activity that correlated with increased cell cycling and apoptosis of HSCs.[13] Levels of reactive oxygen species (ROSs) were intriguingly increased in *FoxO*-deficient HSCs; in vivo treatment with the antioxidative agent *N*-acetyl-L-cysteine (NAC) rescued the *FoxO*-deficient HSC phenotype. Even in mice deficient

Submitted April 4, 2008; accepted July 27, 2008. Prepublished online as *Blood* First Edition paper, October 22, 2008; DOI 10.1182/blood-2008-04-146480.

An Inside *Blood* analysis of this article appears at the front of this issue.

The online version of this article contains a data supplement.

The publication costs of this article were defrayed in part by page charge payment. Therefore, and solely to indicate this fact, this article is hereby marked "advertisement" in accordance with 18 USC section 1734.

for a single *FoxO* gene, *FoxO3a*, much milder but similar defects were observed.[14] These results suggest that FoxOs play essential roles in the establishment of resistance to physiologic oxidative stress, a resistance necessary to ensure the quiescence, survival, and function of HSCs. These findings demonstrate a tight correlation between lipid raft status and Akt-FoxO signaling in the context of HSC hibernation and survival and indicate that LRC plays a key role in HSC emergence from hibernation and that LRC-inhibitory signals from the BM niche are critical in the induction and maintenance of HSC hibernation.

One of the niche signaling molecules, TGF-β, acts as a negative regulator of hematopoietic stem and progenitor cell proliferation in vitro.[7] Upon association with TGF-β, TGF-β type II receptor (TβRII) forms a complex with TGF-β type I receptor (TβRI). Subsequently, the activated TGF-β receptor complex phosphorylates receptor-activated Smads (R-Smad2) and R-Smad3. R-Smads eventually heterodimerize with the common mediator Smad4, and the resulting complex translocates to the nucleus and recruits transcriptional cofactors to control expression of genes, including those involved in the cell cycle. It has been reported that TGF-β1–null mice and inducible TβRII knockout models develop a transplantable lethal inflammatory disorder affecting multiple organs.[15,16] However, mice deficient in the TβRI, activin receptor-like kinase 5 (ALK-5), show no defects in HSC quiescence or in maintenance of the HSC pool.[17] Mice deficient for the TGF-β type II receptor have not been well characterized with respect to HSC hibernation.[16] TGF-β signaling deficiency so far has not revealed any effect on HSC proliferation and differentiation in vivo. Therefore, the outcome of TGF-β signaling is believed to be context dependent in hematopoiesis and the regulation of hematopoietic stem and progenitor cells is more complicated in the BM microenvironment in vivo than is seen in liquid cultures ex vivo.

In this study, we screened candidate niche signals that inhibit lipid raft clustering and identified that TGF-β efficiently inhibits cytokine-mediated LRC. We further characterized its role in HSC hibernation.

Methods

Mice

C57BL/6 (B6-Ly5.2) mice were purchased from Japan SLC (Shizuoka, Japan). C57BL/6 mice congenic for the Ly5 locus (B6-Ly5.1) were purchased from Sankyo-Lab Service (Tsukuba, Japan). C57BL/6 Ly5.1 × Ly5.2 F1 mice were bred and maintained in the Animal Research Facility of the Institute of Medical Science, University of Tokyo. Animal care in our laboratory was in accord with the guidance of Tokyo University for animal and recombinant DNA experiments.

Purification of mouse HSCs and CD34$^+$KSL cells

Mouse CD34$^-$KSL HSCs and CD34$^+$KSL progenitor cells were purified from BM cells of 2-month-old mice. In brief, low-density cells were isolated on Lymphoprep (1.086 g/mL; Nycomed, Oslo, Norway). The cells were stained with an antibody cocktail consisting of biotinylated anti–Gr-1, –Mac-1, –B220, -CD4, -CD8, and –Ter-119 monoclonal antibodies (PharMingen, San Diego, CA). Lineage-positive cells were depleted with antibiotin MicroBeads (Miltenyi Biotec, Bergisch Gladbach, Germany). The remaining cells were further stained with fluorescein isothiocyanate (FITC)–conjugated anti-CD34, phycoerythrin (PE)–conjugated anti–Sca-1, and allophycocyanin (APC)–conjugated anti–c-Kit antibodies (PharMingen). Biotinylated antibodies were detected with streptavidin-APC Cy7 (Molecular Probes, Eugene, OR). Analysis and cell sorting were performed on a MoFlo using Summit software (Dako, Glostrup, Denmark) and results were analyzed with FlowJo software (TreeStar, Ashland, OR).[18]

Immunofluorescent staining and linearization analysis

The markers and antibodies used were the DNA marker 4,6-diamidino-2-phenylindole (DAPI), Alexa-488–conjugated cholera toxin B subunit (CTxB), Alexa-647–conjugated goat anti–rabbit IgG, goat anti–mouse IgG, and Alexa-488–conjugated goat anti–rabbit IgG (Molecular Probes, Carlsbad, CA), rabbit anti–phospho-Akt and rabbit anti-FOXO3a (Upstate Cell Signaling, Charlottesville, VA), rabbit anti-p57 (Santa Cruz Biotechnology, Santa Cruz, CA), rabbit anti–phospho-Smad2/3 (CHEMICON, Temecula, CA), and rabbit anti–phospho-Src (Y418; Biosource, Camarillo, CA). Individual CD34$^-$ KSL cells were sorted into a serum-free culture-medium drop supplemented with 50 ng/mL mouse SCF and/or 50 ng/mL human TPO on slide glasses. The sorted cells were incubated at 37°C for the indicated time periods. After fixation with 2% paraformaldehyde and blocking in 10% goat serum for 1 hour at room temperature, cells were incubated with a primary antibody for 12 hours at 4°C. The cells were then washed and were incubated with a secondary antibody for 30 minutes at room temperature. Immunofluorescence was observed with a Leica TCS SP2 AOBS confocal microscope (Wetzlar, Germany) or with an Olympus Laser Scanning Cytometer 2 (LSC2; Tokyo, Japan).

Single-cell culture

CD34$^-$KSL cells were clonally deposited into 96-well microtiter plates containing 200 μL S-Clone SF-03 (Sanko Junyaku, Tokyo, Japan) supplemented with 5×10^{-5} M 2-β-mercaptoethanol, 10% FCS, and the indicated cytokines (20 ng/mL mouse SCF, 50 ng/mL human TPO, 20 ng/mL mouse IL-3, and 2 U/mL human EPO) in the presence or absence of 5 ng/mL human TGF-β1, TGF-β2, TGF-β3, latent TGF-β1, Activin-A, and Nodal (R&D Systems, Minneapolis, MN). Survival and cell division of HSCs were monitored by microscopy. To allow colony formation, single HSCs were cultured in the presence of SCF, TPO, IL-3, EPO, and anti–TGF-β blocking antibody (R&D Systems) for 11 days. Colonies were recovered, cytospun onto glass slides, and subjected to May-Grünwald-Giemsa staining for morphologic examination.

Competitive repopulation assays

Competitive repopulation assays were performed using the Ly5 system. In brief, single cultured HSCs or pooled single cultured HSCs (B6-Ly5.1) were mixed with 2×10^5 BM competitor cells (B6-F1) and were transplanted into B6-Ly5.2 mice irradiated at a dose of 9.5 Gy. After transplantation, peripheral blood cells of the recipients were stained with biotinylated anti-Ly5.1 (A20) and FITC-conjugated anti-Ly5.2. The cells were simultaneously stained with PE-Cy7–conjugated anti-B220 antibody, a mixture of APC-conjugated anti–Mac-1 and –Gr-1 antibodies, or a mixture of PE-conjugated anti-CD4 and -CD8 antibodies (PharMingen). Biotinylated antibody was developed with streptavidin Alexa-594 (Molecular Probes, Carlsbad, CA). The cells were analyzed on a fluorescence-activated cell sorting (FACS) Vantage (BD. Franklin Lakes, NJ). Percentage chimerism was calculated as (percentage Ly5.1 cells) × 100/(percentage Ly5.1 cells + percentage F1 cells). When percentage chimerism of donor-derived cells was more than 1.0 (summed over myeloid, B-lymphoid, and T-lymphoid lineages), recipient mice were considered to be multilineage reconstituted (positive mice).

RT-PCR

Semiquantitative RT-PCR was carried out using normalized cDNA and quantitative PCR with TaqMan rodent GAPDH control reagent (Perkin-Elmer Applied Biosystems, Foster City, CA) as previously described.[19] Cycling parameters were as follows: denaturation at 95°C for 15 seconds, annealing at 58°C for 15 seconds, and extension at 72°C for 30 seconds. Amplification proceeded for 38 cycles. PCR products were separated on 1.4% agarose gels and visualized by ethidium bromide staining.

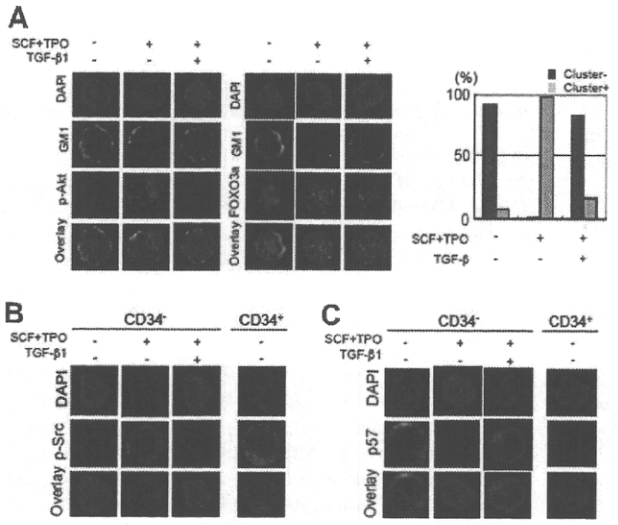

Figure 1. TGF-β inhibits LRC and attenuates cytokine signals. (A) TGF-β inhibits cytokine-mediated LRC and maintains repression of the Akt-FoxO pathway in HSCs. Freshly isolated CD34⁻KSL HSCs were sorted into individual serum-free culture-medium drops on slide glasses. The sorted cells were incubated at 37°C for 30 minutes in the presence or absence of TGF-β1, and then were stimulated with SCF and TPO for another 30 minutes. The cells were stained with DAPI (blue), CTxB (green), and an anti–phospho-Akt (red) or an anti-FoxO3a antibody (red). Proportions of CD34⁻KSL HSCs that showed lipid raft cluster formation are indicated as gray bars (Cluster+; right panel). (B) TGF-β inhibits activation of c-Src in HSCs. Freshly isolated CD34⁻KSL HSCs were incubated in the presence or absence of TGF-β1 for 30 minutes and then were stimulated with SCF and TPO for another 30 minutes. Freshly isolated CD34⁺KSL progenitor cells were also subjected to analysis. The cells were stained with DAPI (blue) and an anti–phospho-c-Src antibody (red). (C) TGF-β maintains cytoplasmic accumulation of p57 in HSCs. Freshly isolated CD34⁻KSL HSCs were incubated in the presence or absence of TGF-β1 for 30 minutes and then were stimulated with SCF and TPO for another 30 minutes. Freshly isolated CD34⁺KSL progenitor cells were also subjected to analysis. The cells were stained with DAPI (blue) and an anti-p57 antibody (green).

Results

TGF-β inhibits LRC and attenuates cytokine signals in HSCs

Whereas HSCs are exposed to a variety of secreted and membrane-bound growth factors in the BM,[3] lipid rafts are diffusely distributed on freshly isolated CD34⁻KSL HSCs but are highly polarized or clustered on CD34⁺KSL progenitor cells.[9] This suggests that LRC is tightly inhibited on HSCs in the BM niche. We hypothesized that some signals from the niche act against LRC and keep HSCs in hibernation. Several niche signals are associated with HSC dormancy. These include the Ang-1–Tie-2 signal, the Notch ligand–Notch signal, the N-cadherin homotypic signal, the TGF-β signal, and so on. We tested the effects of these signals on LRC in HSCs.

Lipid raft distribution was assessed using cholera toxin subunit B (CTxB) to label endogenous GM1 ganglioside, a component of lipid rafts. Freshly isolated CD34⁻KSL HSCs were incubated with Ang-1, TGF-β1, or the Notch ligand Jagged-1 for 1 hour, and were then stimulated with SCF and TPO, cytokines supportive of HSC self-renewal and survival, for 30 minutes. As reported, stimulation of HSCs by cytokines induced LRC. Jagged-1 had no antagonistic effect at all on LRC. Ang-1 partially inhibited LRC, but not enough to inhibit activation of the Akt-FoxO pathway and to induce cell-cycle arrest (data not shown). In contrast, TGF-β strikingly inhibited SCF- and TPO-induced LRC (Figure 1A). TGF-β1 also inhibited Akt activation and caused sustained nuclear accumulation of FOXO3a (Figure 1A). Lipid raft protein components include transmembrane antigens/receptors, GPI-anchored proteins, cytoskeletal proteins, Src-family kinases, G-proteins, and other proteins involved in signal transduction. Treatment of HSCs with PP2, an inhibitor specific for Src-family kinases, inhibited LRC (Figure S1, available on the *Blood* website; see the Supplemental Materials link at the top of the online article). Intriguingly, TGF-β1 similarly suppressed the cytokine-mediated activation of c-Src tyrosine kinase (Figure 1B). Hibernating HSCs express high levels of cytoplasmic cyclin D1 and p57 cyclin–dependent kinase inhibitor (CDKI). Cytokine stimulation induces nuclear translocation of cyclin D1 and disappearance of p57, which is supposedly due to rapid protein degradation.[9] TGF-β1 inhibited nuclear translocation of cyclin D1 (data not shown) and kept p57 in the cytoplasm (Figure 1C). These effects of TGF-β1 on HSCs were comparable with that of β-cyclodextrin (MβCD), which inhibits LRC by depleting plasma membrane cholesterol.[9]

TGF-β induces HSC hibernation ex vivo

We then asked whether TGF-β induces quiescence in HSCs. Single CD34⁻KSL HSCs were cultured in the presence of SCF, TPO, and TGF-β1. In the presence of SCF and TPO, more than 85% of HSCs proliferated robustly, but in the absence of SCF or TPO, none survived more than 24 hours (data not shown). In contrast, addition of TGF-β1 in culture strongly suppressed colony formation of single HSCs in a dose-dependent manner (Figure S2). Detailed observation revealed that addition of 5 ng/mL TGF-β1 in culture strongly suppressed division of single HSCs that, however, remained alive. During 5-day culture, 57% of single HSCs stayed dormant, that is, persisted as living single cells, and 22% of single HSCs divided only once (Figure 2A). Similar results were obtained when HSCs were cultured under another HSC-supporting cytokine condition, SCF plus IL-11 (Figure S3). After culture medium was changed to an optimal medium supplemented with SCF, TPO, IL-3, and EPO, 72.2% of single HSCs, which had stayed dormant for 5 days, gave rise to colonies; of these, 47% were neutrophil/macrophage/erythroblast/megakaryocyte (nmEM) colonies, derived from colony-forming units–nmEM (CFU-nmEMs) with multipotency, that is, a full range of differentiation capacity along myeloid lineages (Figure 2B). Thus, 33.9% of surviving single HSCs could retrospectively be inferred to have been CFU-nmEMs. Even after 7 days of culture, most single HSCs retained multipotency (Figure 2B). These data demonstrate that TGF-β can keep HSCs in hibernation without loss of higher-order biologic potential ex vivo. Furthermore, when we compared the activities of TGF-β1, TGF-β2, and TGF-β3 with respect to induction of the hibernating state, some HSCs survived as single cells for more than 15 days in culture in the presence of TGF-β3 (Figure S4).

To obtain direct evidence of HSC activity, we performed competitive hematopoiesis repopulation assays in vivo. We again selected single HSCs that had not divided during 5-day clonal single-cell culture in the presence of SCF, TPO, and TGF-β. Single HSCs or pools comprising 20 individual HSCs were transplanted into lethally irradiated recipient mice. As a control, freshly isolated single HSCs or pools comprising 20 individual HSCs were similarly transplanted. Comparable proportions of freshly isolated and cultured hibernating (in the presence of TGF-β) single HSCs exhibited LTR activity (26% and 20%, respectively); establishment of chimerism also was comparable (13.5% and 9.5%, respectively) (Figure 2C). In contrast, when single HSCs were cultured in the presence of SCF and TPO without TGF-β, they robustly proliferated but lost LTR activity (data not shown). All recipient mice infused with pools of 20 freshly isolated HSCs showed donor cell repopulation. So did those infused with pools of 20 cultured single

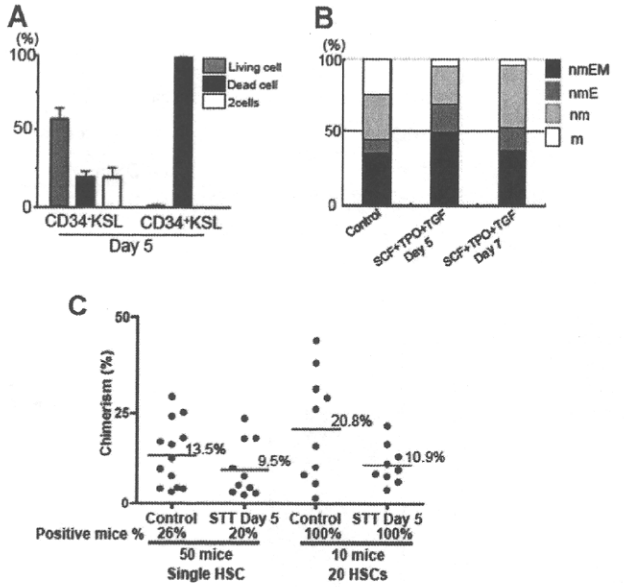

Figure 2. TGF-β induces HSC hibernation ex vivo. (A) Freshly isolated CD34⁻KSL HSCs and CD34⁺KSL hematopoietic progenitor cells were sorted clonally into 96-well microtiter plates and incubated in the presence of SCF, TPO, and TGF-β1. At day 5 of culture, cell viability and cell numbers were assessed under an inverted microscope. (B) Freshly isolated CD34⁻KSL HSCs were sorted clonally into 96-well microtiter plates and incubated in the presence of SCF, TPO, and TGF-β1. At the indicated time points, surviving single HSCs that had not divided were selected. Culture medium was replaced with one supplemented with SCF, TPO, IL-3, and EPO, permitting colony formation. After 14 subsequent days of culture, the colonies were recovered for morphologic examination. As a control, freshly isolated CD34⁻KSL HSCs were sorted clonally into 96-well microtiter plates supplemented with SCF, TPO, IL-3, and EPO and cultured for 14 days. Proportions of colony types are depicted: n indicates neutrophils; m, macrophages; E, erythroblasts; and M, megakaryocytes. (C) Freshly isolated CD34⁻KSL HSCs were sorted clonally into 96-well microtiter plates and were incubated in the presence of SCF, TPO, and TGF-β1. At day 5 of culture, surviving single HSCs that had not divided during 5-day culture were selected. Single HSCs or pools of 20 single HSCs (indicated by STT day 5; B6-Ly5.1) were mixed with B6-Ly5.2 competitor cells and injected into lethally irradiated B6-Ly5.2 recipient mice. As a control, freshly isolated single-HSC or 20-HSCs pools were similarly transplanted into recipient mice. Percentage chimerism of donor cells in recipient mice 12 weeks after transplantation is plotted as dots, with mean values indicated as bars. Recipient mice with donor cell chimerism more than 1.0% for myeloid and for B- and T-lymphoid lineages were considered multilineage reconstituted (positive mice).

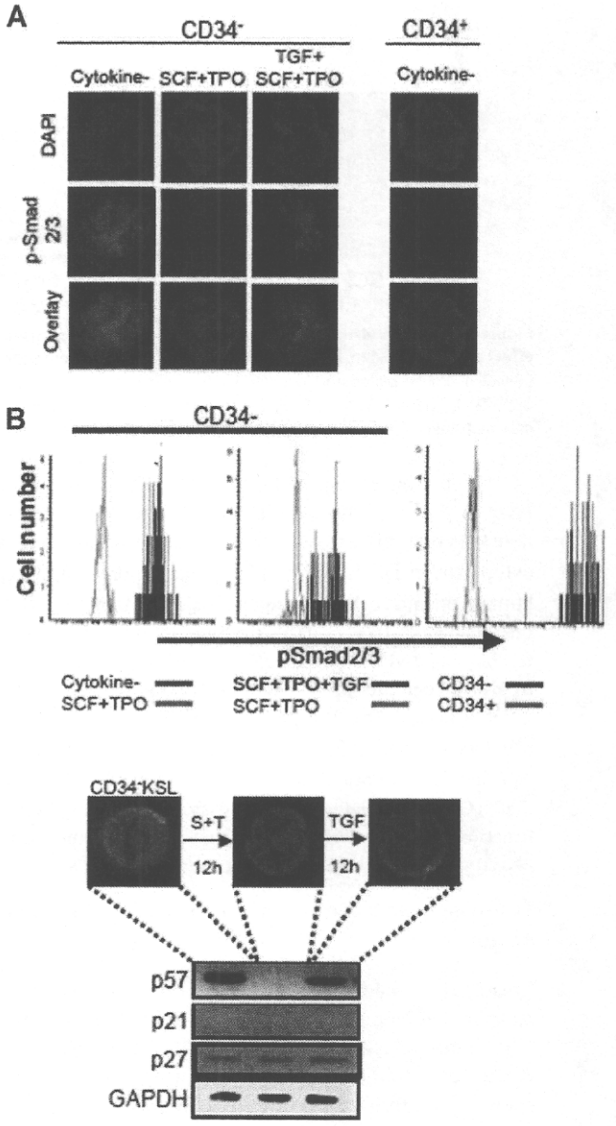

Figure 3. TGF-β signaling is highly active in dormant HSCs and regulates *p57* expression. (A) Active TGF-β signaling in HSCs demonstrated by presence of phosphorylated Smad2/3 in the nucleus. Freshly isolated CD34⁻KSL HSCs (CD34⁻) and CD34⁺KSL hematopoietic progenitor cells (CD34⁺) were sorted in a serum-free culture-medium drop on slide glasses. The sorted cells were incubated at 37°C for 30 minutes in the presence or absence of TGF-β1 and then were stimulated with SCF and TPO for another 30 minutes. Freshly isolated CD34⁺KSL progenitor cells were also subjected to analysis. The cells were stained with DAPI (blue) and an anti–phospho-Smad2/3 antibody (red). Representative images are depicted on the top panels. In the bottom panels, the levels of immunofluorescence quantitated by an Olympus Laser Scanning Cytometer 2 (LSC2) are depicted. X- and y-axes are indicated in logarithmic and linear scales, respectively. The left panel presents data from freshly isolated CD34⁻KSL HSCs (CD34⁻) incubated for 30 minutes in the presence or absence of SCF and TPO. The middle panel presents data from freshly isolated CD34⁻KSL HSCs (CD34⁻) incubated for 30 minutes in the presence or absence of TGF-β1, and then stimulated with SCF and TPO for another 30 minutes. The right panel presents data from freshly isolated CD34⁻KSL HSCs (CD34⁻) and CD34⁺KSL hematopoietic progenitor cells (CD34⁺). (B) TGF-β up-regulates *p57* gene expression in HSCs to induce cell-cycle arrest. Freshly isolated CD34⁻KSL HSCs were incubated in the presence of SCF (S) and TPO (T) for 12 hours, and were cultured for another 12 hours in the presence of TGF-β1 (TGF) in addition to SCF and TPO. The cells were stained with DAPI (blue) and an anti-p57 antibody (green). mRNA expression of mouse *Cip/Kip* genes was analyzed for each cell (bottom panel).

HSCs, although established chimerism declined compared with that established by freshly isolated HSCs. All these data strongly support the proposition that TGF-β induces hibernation in HSCs ex vivo without affecting HSC capacity to self-renew and to differentiate into a full range of hematopoietic cell lineages.

The TGF-β signal is active in hibernating niche HSCs

The activated TGF-β receptor complex phosphorylates Smad2 and Smad3. Smad2 and Smad3 use Smad4 as a partner to form a transcriptionally active complex. To obtain physiologic evidence that supports active TGF-β signaling in niche HSCs, we next examined TGF-β signals in freshly isolated HSCs. Smad2/3, the signaling molecules directly downstream from and activated by TGF-β receptors, were highly phosphorylated in freshly isolated CD34⁻KSL HSCs, where they accumulated in the nucleus. In contrast, Smad2/3 were scarcely phosphorylated in CD34⁺KSL progenitor cells (Figure 3A). Quantification of the levels of Smad2/3 phosphorylation by laser scanning microscopy showed a striking contrast between freshly isolated CD34⁻KSL HSCs and CD34⁺KSL progenitors (Figure 3A). These data strongly indicate that the TGF-β signaling pathway is active in HSCs in the BM niche, but not in progenitor cells. We observed, in keeping with this, that Smad2/3 in HSCs were rapidly dephosphorylated by cytokine stimulation. Pretreatment of HSCs with TGF-β, however, again counteracted cytokine stimulation and Smad2/3 remained phosphorylated (Figure 3A).

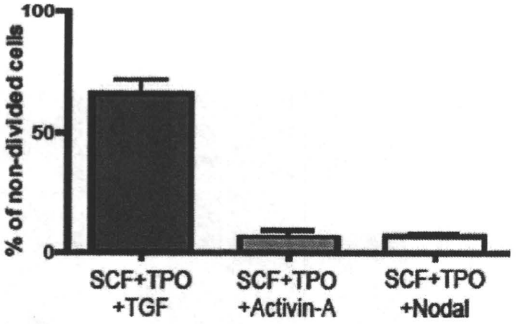

Figure 4. TGF-β, but not other TGF-β family members, confers a cytostatic effect on HSCs ex vivo. Freshly isolated CD34⁻KSL HSCs were sorted clonally into 96-well microtiter plates and incubated in the presence of SCF, TPO, and TGF-β1; SCF, TPO, and Activin-A; or SCF, TPO, and Nodal. At day 2 of culture, nondivided cells that stayed dormant were assessed under an inverted microscope.

We previously reported that CD34⁻KSL HSCs express a high level of *p57*^{Kip2}, whereas CD34⁺KSL progenitor cells do not. Of note was that p57 as well as cyclin D1, D2, and D3 localize in the cytoplasm in HSCs.[9] That TGF-β up-regulates *p57* expression in human primitive hematopoietic cells to induce cell-cycle arrest intrigued us.[20] To verify this finding in mouse HSCs, we stimulated freshly isolated CD34⁻KSL HSCs with SCF and TPO for 12 hours, to down-regulate *p57;* we then treated the cells with TGF-β. Twelve hours after the addition of TGF-β, p57 was abundantly reinduced at both mRNA and protein levels, whereas expression of *p21* and *p27* did not change at all (Figure 3B). These data indicate that TGF-β regulates the expression of p57, which supposedly functions as a specific CDKI that binds to and suppresses the activity of the cyclin D/CDK complexes in HSCs.

TGF-β induces hibernation, but other TGF-β family members do not

Smad2 and Smad3 are activated not only by TGF-β, but also by Activin and Nodal.[21] We evaluated the effects of these agents on HSC cell cycle. Single CD34⁻KSL HSCs were cultured in the presence of SCF, TPO, and Activin or Nodal. TGF-β strongly suppressed division of single HSCs; 65.7% of them stayed dormant during 2-day culture. Activin-A and Nodal were not efficient in suppressing division of single HSCs; they, respectively maintained dormancy in only 6.6% and 6.9% of HSCs during 2-day culture (Figure 4). These data establish that within its family TGF-β has a major role in maintenance of HSC hibernation.

Activation of latent TGF-β is required for TGF-β bioactivity

TGFβ reportedly is produced not only by niche cells, but also by HSCs themselves.[7] As expected, HSCs expressed a significant level of *TGF-β1* and a low level of *TGF-β3,* but not *Activin A* or *Nodal,* indicating the presence of both autocrine and paracrine regulatory loops of TGF-β signaling (Figure 5A). Importantly, however, TGF-β is produced as an inactive form, latent TGF-β. We asked whether HSCs themselves could activate latent TGF-β to establish an autocrine TGF-β signaling loop. We seeded single CD34⁻KSL HSCs in the presence of SCF and TPO along with either active-form TGF-β or latent TGF-β, and allowed the HSCs to form colonies. TGF-β strongly suppressed colony formation, whereas latent TGF-β did not affect colony formation at all. These data indicate that HSCs can produce latent TGF-β but cannot activate it by themselves. Since TGF-β is produced by a variety of cells as an inactive form, the capacity to activate latent TGF-β could be a key property of BM niche cells.

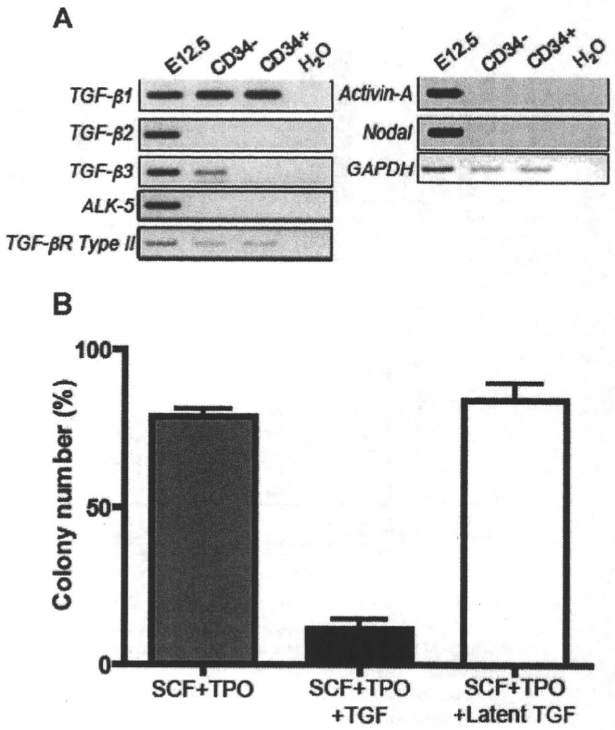

Figure 5. Activation of latent TGF-β is required for TGF-β bioactivity on HSCs. (A) mRNA expression of TGF-β family member genes was analyzed for total embryo at E12.5, freshly isolated BM CD34⁻KSL HSCs (CD34⁻), and CD34⁺KSL hematopoietic progenitor cells (CD34⁺). (B) Freshly isolated CD34⁻KSL HSCs (CD34⁻) were sorted clonally into 96-well microtiter plates and incubated in the presence of SCF and TPO along with either TGF-β1 or latent TGF-β1, and were allowed to form colonies. After 14 subsequent days of culture, the numbers of colonies were counted and the percentages of starting HSCs that gave rise to colonies were presented.

Discussion

The cell-cycle status of HSCs in the niche is supposed to be precisely regulated by a specific combination of niche signals. We have reported an unexpected role of lipid raft organization in the maintenance of HSC hibernation through regulating the PI3K-Akt-FoxO pathway that lies downstream of cytokine signaling.[9] HSCs are exposed to a variety of secreted and membrane-bound growth factors in the niche. Nonetheless, our findings clearly demonstrate that lipid raft reorganization is strictly inhibited in HSCs in the niche. We inferred that nonclustered lipid raft microdomains finely tune cytokine signals and mediate them toward suitability for HSC survival in the hibernating state, and that some niche signals inhibit lipid raft reorganization to maintain HSC hibernation. These findings support a novel model in which HSC fate, that is, hibernation or cell-cycle re-entry, largely depends on lipid raft regulation.

We have now identified that TGF-β inhibits cytokine-induced LRC (Figure 1A). TGF-β suppresses Akt activation and induces nuclear accumulation of FoxO3a in HSCs. It also inhibits translocation of cyclin D1 into the nucleus and maintains high cytoplasmic accumulations of p57 (Figure 1D and data not shown). Through these mechanisms, TGF-β strongly inhibits cell division and maintains HSCs in the hibernating state ex vivo. Together with our finding that Smad2 and Smad3, which are activated by the TGFβ receptor complex, are selectively and highly phosphorylated in CD34⁻KSL HSCs, but not in CD34⁺KSL progenitor cells, these findings strongly indicate a physiologic role for TGF-β in HSC hibernation in the

niche (Figure 3A). This notion is also supported by the study of *C elegans*, which indicated a critical role of Daf-7 as a positive regulator of Daf-16.[22] Daf-7 is a TGF-β–like molecule. Via its receptor and downstream signaling molecules (Daf-4, Daf-1, Daf-8, and Daf-14), it up-regulates Daf-16 expression and exerts a dauer larval gene program.[23]

TGF-β is widely expressed in BM by elements that include osteoblasts and other stromal cells. Importantly, however, TGF-β is produced as a latent form. Latent TGF-β must be processed and activated. As shown in Figure 5B, HSCs are not able to activate latent TGF-β. That the BM niche is where TGF-β can be processed/activated and where TGF-β induces HSC hibernation is thus a tempting hypothesis. In contrast, Ang-1, another regulator of HSC hibernation, was much less effective than TGF-β in inhibiting cytokine-induced LRC and subsequent Akt activation (data not shown). Recently, the TPO signal was proposed as an essential component for HSC hibernation in the osteoblastic niche.[24] TPO efficiently induces LRC and activates the PI3K-Akt pathway in vitro. However, its signal is supposedly attenuated by inhibited LRC in hibernating HSCs in the niche. We assume that the attenuated TPO signal by inhibitory niche signals including TGF-β acts as a survival signal but not proliferation signal on HSCs and holds the key in keeping HSCs in hibernation. These data highlight lipid raft assembly and its regulation by TGF-β as a novel regulatory component of HSC hibernation. Our findings thus indicate that HSC hibernation is regulated by at least 2 different routes, the Ang-1–Tie-2 and TGF-β–Smad signaling pathways, and establish a central role for TGF-β in regulating the lipid raft–PI3K–Akt–FOXO pathway.

Although TGF-β has been well characterized as a negative regulator of hematopoietic stem and progenitor cell proliferation in vitro,[7] mice models deficient for TGF-β signaling molecules, including ALK-5 TβRI, show no defects in maintenance or quiescence of HSCs.[17] These discrepancies may be at least partly explained by the considerably low mRNA expression of ALK-5 in HSCs compared with that in E12.5 total embryo (Figure 5A), which is indicative of alternative TβRIs in HSCs. Mice deficient for the TβRII have not been well characterized with respect to HSC hibernation because of lethal inflammatory disorder affecting multiple organs.[16] Furthermore, overlapping receptor and Smad usage by different TGF-β superfamily ligands (TGF-βs, BMPs, and Activins) accounts for their functional redundancies, making their signals more complicated in vivo than is seen in liquid cultures ex vivo. Of note is that Smad4, which acts at a common level of convergence for all TGF-β superfamily signals, has recently been identified as critical for maintenance of self-renewing HSCs.[25] Thus, the physiological role of the TGF-β awaits further evaluation.

The negative regulation of lipid raft assembly is poorly understood. In this regard, the direct inhibition of lipid raft reorganization by TGF-β is notable. In the present study, TGF-β significantly inhibited cytokine-induced activation of c-Src, one of the lipid raft components, in HSCs (Figure 1B). This effect was comparable with that exerted by PP2, an inhibitor specific for Src-family kinases (Figure S1). Intriguingly, TGF-β has been reported to down-regulate protein expression of Src-family kinases.[26,27] Although the precise mechanism whereby TGF-β inhibits c-Src activation remains obscure, Src-family kinases could be key targets for TGF-β in affecting lipid raft reorganization.

TGF-β reportedly induces cell cycle arrest through up-regulating CDKIs, including p15INK4B (p15), p21, and p27, in various cell types.[28,29] However, TGF-β has been demonstrated to induce growth arrest in HSCs independently of p21 or p27.[30] We here have presented evidence that TGF-β specifically up-regulates the expression of *p57*, but not *p15*, *p21*, or *p27*, in HSCs (Figure 3B and data not shown). In accord with our findings, *p57* has been identified as the only CDKI significantly up-regulated by TGF-β in vitro in human $CD34^+$ primitive hematopoietic cells; of importance was the observation that knockdown of *p57* expression blocked the cytostatic effect of TGF-β.[20] All these findings indicate the importance of TGF-β in regulating *p57* expression and in maintaining HSC hibernation.

In this study, we also evaluated the role of autocrine TGF-β signaling loop in HSCs. Our data indicated that HSCs can produce latent TGF-β but cannot activate it by themselves. Latent TGF-β does not affect HSC cell growth at all. Intriguingly, a cell cycle–independent role of autocrine TGF-β has been reported on human primitive hematopoietic progenitor cells under a culture condition without supporting cells that can activate latent TGF-β.[31] Whether the latent TGF-β can transduce alternative signals via an as-yet-unrecognized pathway in HSCs is a tempting question to be addressed.

Our findings stress the critical role of lipid rafts in regulating the cell-cycle status of HSCs and demonstrate a novel interplay between the lipid raft–PI3K–Akt–FoxO and the TGF-β–Smad signaling pathways in HSCs hibernating in the BM niche. Smad proteins activated by TGF-β could form a complex with FoxO proteins FoxO1, FoxO3a, and FoxO4.[32] TGF-β–mediated interaction between these 2 signaling pathways thus could hold a key role in the regulation of gene expression that controls HSC hibernation.

Acknowledgments

We thank Y. Morita and Y. Yamazaki for technical help and advice and Dr A. S. Knisely for critical reading of the paper.

This work was supported in part by grants from the Ministry of Education, Culture, Sport, Science and Technology, Japan, Japan Science and Technology Corporation (JST), the Naito Foundation (Tokyo, Japan), and the Terumo Lifescience Foundation (Kanagawa, Japan).

Authorship

Contribution: S.Y., A.I., and H.E. designed the research and analyzed data; S.Y., A.I., and H.N. wrote the paper; K.E. contributed vital new reagents; and S.Y. and S.T. performed research and analyzed data.

Conflict-of-interest disclosure: The authors declare no competing financial interests.

Correspondence: Hiromitsu Nakauchi, 4-6-1 Shirokanedai, Minato-ku, Tokyo, Japan; e-mail: nakauchi@ims.u-tokyo.ac.jp.

References

1. Cheshier SH, Morrison SJ, Liao X, Weissman IL. In vivo proliferation and cell cycle kinetics of long-term self-renewing hematopoietic stem cells. Proc Natl Acad Sci U S A. 1999;96:3120-3125.
2. Sudo K, Ema H, Morita Y, Nakauchi H. Age-associated characteristics of murine hematopoietic stem cells. J Exp Med. 2000;192:1273-1280.
3. Taichman RS. Blood and bone: two tissues whose fates are intertwined to create the hematopoietic stem-cell niche. Blood. 2005;105:2631-2639.
4. Arai F, Hirao A, Ohmura M, et al. Tie2/angiopoietin-1 signaling regulates hematopoietic stem cell quiescence in the bone marrow niche. Cell. 2004; 118:149-161.
5. Calvi LM, Adams GB, Weibrecht KW, et al. Osteoblastic cells regulate the haematopoietic stem cell niche. Nature. 2003;425:841-846.
6. Zhang J, Niu C, Ye L, et al. Identification of the haematopoietic stem cell niche and control of the niche size. Nature. 2003;425:836-841.

7. Larsson J, Karlsson S. The role of Smad signaling in hematopoiesis. Oncogene. 2005;24:5676-5692.
8. Osawa M, Hanada K, Hamada H, Nakauchi H. Long-term lymphohematopoietic reconstitution by a single CD34-low/negative hematopoietic stem cell. Science. 1996;273:242-245.
9. Yamazaki S, Iwama A, Takayanagi S, et al. Cytokine signals modulated via lipid rafts mimic niche signals and induce hibernation in hematopoietic stem cells. EMBO J. 2006;25:3515-3523.
10. Jahn T, Seipel P, Urschel S, Peschel C, Duyster J. Role for the adaptor protein Grb10 in the activation of Akt. Mol Cell Biol. 2002;22:979-991.
11. Coffer PJ, Burgering BM. Forkhead-box transcription factors and their role in the immune system. Nat Rev Immunol. 2004;4:889-899.
12. Greer EL, Brunet A. FOXO transcription factors at the interface between longevity and tumor suppression. Oncogene. 2005;24:7410-7425.
13. Tothova Z, Kollipara R, Huntly BJ, et al. FoxOs are critical mediators of hematopoietic stem cell resistance to physiologic oxidative stress. Cell. 2007;128:325-339.
14. Miyamoto K, Araki KY, Naka K, et al. Foxo3a is essential for maintenance of the hematopoietic stem cell pool. Cell Stem Cell. 2007;1:101-112.
15. Shull MM, Ormsby I, Kier AB, et al. Targeted disruption of the mouse transforming growth factor-beta 1 gene results in multifocal inflammatory disease. Nature. 1992;359:693-699.
16. Levéen P, Larsson J, Ehinger M, et al. Induced disruption of the transforming growth factor β type II receptor gene in mice causes a lethal inflammatory disorder that is transplantable. Blood. 2002;100:560-568.
17. Larsson J, Blank U, Helgadottir H, et al. TGF-beta signaling-deficient hematopoietic stem cells have normal self-renewal and regenerative ability in vivo despite increased proliferative capacity in vitro. Blood. 2003;102:3129-3135.
18. Ema H, Morita Y, Yamazaki S, et al. Adult mouse hematopoietic stem cells: purification and single-cell assays. Nat Protoc. 2006;1:2979-2987.
19. Osawa M, Yamaguchi T, Nakamura Y, et al. Erythroid expansion mediated by the Gfi-1B zinc finger protein: role in normal hematopoiesis. Blood. 2002;100:2769-2777.
20. Scandura JM, Boccuni P, Massague J, Nimer SD. Transforming growth factor beta-induced cell cycle arrest of human hematopoietic cells requires p57KIP2 up-regulation. Proc Natl Acad Sci U S A. 2004;101:15231-15236.
21. Waite KA, Eng C. From developmental disorder to heritable cancer: it's all in the BMP/TGF-beta family. Nat Rev Genet. 2003;4:763-773.
22. Ogg S, Paradis S, Gottlieb S, et al. The Fork head transcription factor DAF-16 transduces insulin-like metabolic and longevity signals in C. elegans. Nature. 1997;389:994-999.
23. Inoue T, Thomas JH. Suppressors of transforming growth factor-beta pathway mutants in the Caenorhabditis elegans dauer formation pathway. Genetics. 2000;156:1035-1046.
24. Yoshihara H, Arai F, Hosokawa K, et al. Thrombopoietin/MPL signaling regulates hematopoietic stem cell quiescence and interaction with the osteoblastic niche. Cell Stem Cell. 2007;1:685-697.
25. Karlsson G, Blank U, Moody JL, et al. Smad4 is critical for self-renewal of hematopoietic stem cells. J Exp Med. 2007;204:467-474.
26. Atfi A, Drobetsky E, Boissonneault M, Chapdelaine A, Chevalier S. Transforming growth factor beta down-regulates Src family protein tyrosine kinase signaling pathways. J Biol Chem. 1994;269:30688-30693.
27. Park SS, Eom YW, Kim EH, et al. Involvement of c-Src kinase in the regulation of TGF-beta1-induced apoptosis. Oncogene. 2004;23:6272-6281.
28. Cheng T, Rodrigues N, Shen H, et al. Hematopoietic stem cell quiescence maintained by p21cip1/waf1. Science. 2000;287:1804-1808.
29. Ezoe S, Matsumura I, Satoh Y, Tanaka H, Kanakura Y. Cell cycle regulation in hematopoietic stem/progenitor cells. Cell Cycle. 2004;3:314-318.
30. Cheng T, Shen H, Rodrigues N, Stier S, Scadden DT. Transforming growth factor beta 1 mediates cell-cycle arrest of primitive hematopoietic cells independent of p21(Cip1/Waf1) or p27(Kip1). Blood. 2001;98:3643-3649.
31. Pierelli L, Marone M, Bonanno G, et al. Modulation of bcl-2 and p27 in human primitive proliferating hematopoietic progenitors by autocrine TGF-beta1 is a cell cycle-independent effect and influences their hematopoietic potential. Blood. 2000;95:3001-3009.
32. Seoane J, Le HV, Shen L, Anderson SA, Massague J. Integration of Smad and forkhead pathways in the control of neuroepithelial and glioblastoma cell proliferation. Cell. 2004;117:211-223.

Stepwise Development of Hematopoietic Stem Cells from Embryonic Stem Cells

Kenji Matsumoto[1], Takayuki Isagawa[2], Toshinobu Nishimura[1], Takunori Ogaeri[1], Koji Eto[1], Satsuki Miyazaki[3], Jun-ichi Miyazaki[3], Hiroyuki Aburatani[2], Hiromitsu Nakauchi[1]*, Hideo Ema[1]*

1 Division of Stem Cell Therapy, Center for Stem Cell and Regenerative Medicine, Institute of Medical Science, University of Tokyo, Tokyo, Japan, **2** Genome Science Division, Research Center for Advanced Science and Technology, University of Tokyo, Tokyo, Japan, **3** Division of Stem Cell Regulation Research, Osaka University Graduate School of Medicine, Osaka, Japan

Abstract

The cellular ontogeny of hematopoietic stem cells (HSCs) remains poorly understood because their isolation from and their identification in early developing small embryos are difficult. We attempted to dissect early developmental stages of HSCs using an *in vitro* mouse embryonic stem cell (ESC) differentiation system combined with inducible HOXB4 expression. Here we report the identification of pre-HSCs and an embryonic type of HSCs (embryonic HSCs) as intermediate cells between ESCs and HSCs. Both pre-HSCs and embryonic HSCs were isolated by their c-Kit$^+$CD41$^+$CD45$^-$ phenotype. Pre-HSCs did not engraft in irradiated adult mice. After co-culture with OP9 stromal cells and conditional expression of HOXB4, pre-HSCs gave rise to embryonic HSCs capable of engraftment and long-term reconstitution in irradiated adult mice. Blast colony assays revealed that most hemangioblast activity was detected apart from the pre-HSC population, implying the early divergence of pre-HSCs from hemangioblasts. Gene expression profiling suggests that a particular set of transcripts closely associated with adult HSCs is involved in the transition of pre-HSC to embryonic HSCs. We propose an HSC developmental model in which pre-HSCs and embryonic HSCs sequentially give rise to adult types of HSCs in a stepwise manner.

Citation: Matsumoto K, Isagawa T, Nishimura T, Ogaeri T, Eto K, et al. (2009) Stepwise Development of Hematopoietic Stem Cells from Embryonic Stem Cells. PLoS ONE 4(3): e4820. doi:10.1371/journal.pone.0004820

Editor: Catherine M. Verfaillie, KU Leuven, Belgium

Received November 5, 2008; **Accepted** January 31, 2009; **Published** March 16, 2009

Funding: This work was supported by grants from the Ministry of Education, Culture, Sport, Science, and Technology, Japan. These grants have no financial interests, and played no role in study and preparation of the manuscript.

Competing Interests: The authors have declared that no competing interests exist.

* E-mail: nakauchi@ims.u-tokyo.ac.jp (HN); hema@ims.u-tokyo.ac.jp (HE)

Introduction

Mammalian hematopoiesis develops in three distinct waves consisting of primitive hematopoiesis, definitive but transient hematopoiesis, and definitive and persistent hematopoiesis which is established by hematopoietic stem cells (HSCs) [1,2]. Both the first and second hematopoietic waves originate from the yolk sac where hemangioblasts, common precursors of the hematopoietic and endothelial lineages likely play a crucial role [3]. However, whether HSCs arise in either the yolk sac or the paraaortic splanchnopleure/aorta-gonad-mesonephros (P-Sp/AGM) region remains controversial [4,5,6]. The relationship between HSCs and hemangioblasts is also obscure [2,7]. In order to understand how HSCs develop in early embryos, it is important to determine the cellular origin of HSCs rather than the organ origin of HSCs.

Hematopoiesis and vasculogenesis in the early mouse embryo have been recapitulated well by *in vitro* ES differentiation systems [8,9,10]. However, generation of HSCs in substantial numbers from ESCs *in vitro* has been difficult. Kyba *et al.* were the first to report that HSCs can be efficiently generated from ESCs in the OP9 co-culture system by combining this with an inducible HOXB4 expression system (OP9 and iHOXB4 system) [11].

In concept, mesodermal cells first commit to the hematopoietic lineage before giving rise to HSCs. We provisionally called such cells pre-HSCs, and attempted to identify them in embryoid bodies (EB) using the OP9 and iHOXB4 system. We detected the potential to give rise to HSCs among c-Kit$^+$CD41$^+$CD45$^-$ cells derived from ESCs on day 6 of culture (EB6). The presence of hematopoietic progenitor activity in this population has been described [12,13,14]. The present report, however, is the first to document the presence of pre-stem cell activity but little hemangioblast activity in the c-Kit$^+$CD41$^+$CD45$^-$ cell population.

Pre-HSCs gave to an embryonic type of HSCs (embryonic HSCs) capable of reconstituting adult hematopoietic system but at a low degree. OP9 cells supported the transition of pre-HSCs to embryonic HSCs. Some genes were up- and down-regulated during the transition via enforced expression of HOXB4. Interestingly, about two-thirds of the markedly up-regulated genes were also found in our adult HSCs gene expression data. These results suggest that adult HSC-related molecules establish the very early stages of HSC development. Based on these results, we propose an HSC development model in which pre-HSCs through the stage of embryonic HSCs give rise to adult types of HSCs.

Results

Experimental design

Our basic experimental strategy consisted of EB formation, co-culture with OP9 cells, and functional assays (Fig. 1). iHOXB4 ESCs were allowed to differentiate spontaneously into EBs for 6 days without HOXB4 expression. We decided to fractionate EB6 cells mainly because by day 6 of culture the number of multipotent